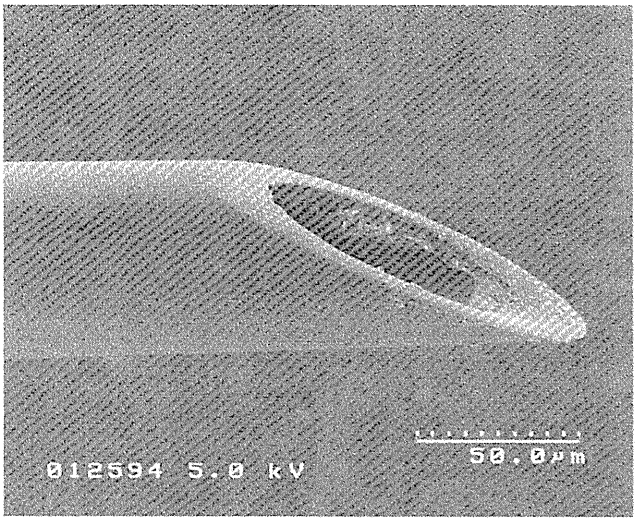

FIGURE 3. The electron microscope of the microneedle shows that the cutting plane of the needle is designed to have a 30° angle. Bar, 50 μm.

micropipette was damaged by the delicate movement of the instrument during the injection procedure. The piercing success rate was 40% (8/20 eyes), and the injection success rate was 25% (5/20 eyes).

The specimen was then embedded in paraffin, with the cut edge marked for keratome sectioning. For a distance of 1000 to 1500 μm spanning the vessel piercing site, every fifth section was mounted. Histologic examination of all eyes in which the microneedle procedure was successful demonstrated that the vascular penetration site and the other retinal vascular wall was clear but the site of the piercing was not damaged (Fig. 5). On the other hand, in all eyes pierced with a micropipette, the wall was severely damaged, the laceration was not clearly identified, and vitreous hemorrhages were seen (Fig. 6).

DISCUSSION

In this study, the microvessels were completely punctured with microneedles and the solution was successfully injected. On the other hand, it was difficult to pierce the vessels with the micropipettes, which easily broke, and the maneuvers were very complicated. The results showed that the microneedles that had been fabricated were more feasible instruments for microvascular surgery than the micropipettes.

TABLE 1. Summary of Results

Procedure	Number of Successful Procedures/ Total Procedures	
	Micropipette	Microneedle
Retinal vein piercing	8/20 (40%)	20/20
Retinal vein injection	5/20 (25%)	20/20

The microfabricated needles used in this study have several advantages over micropipettes, and those advantages may have contributed to the more favorable results. The greatest advantage of the microneedles is their rigidity, because they are made of stainless steel. Even if there is some movement or distortion during the piercing or the injection procedure, they hardly ever break. Moreover, the tip of the microneedle can be easily seen during the piercing procedure, whereas the tip of micropipettes is hard to see, because it is transparent and glistens. Furthermore, the microneedles are fabricated to be attached to the angled handle-shaft shown in Figure 1, which enables a smooth approach to retinal veins.

Micropipettes are used to physically interact with microscopic structures, such as during microinjection and patch clamping procedures.[20] Most micropipettes are made of borosilicate, aluminosilicate, or quartz, and many types and sizes of glass tubing are available. Because of the above characteristics, they have also been used for retinal endovascular surgery for a decade,[3-13] but they have several disadvantages, including fragility and poor visibility.[11-13] In recent years microneedles having diameters as small as 5 μm have been fabricated in the electronics industry[21-23] and they appeared to be quite suitable for use in microvascular surgery. In our experimental studies, all retinal vessels pierced with microneedles were smoothly pierced, and a solution was injected into the microvessel. Also, microneedles are easy to maneuver during eye surgery because of their rigidity.

The results of the histologic examination in this study showed that the cutting plane of the retinal vessel walls pierced with the micropipettes was rougher and more severely damaged than the walls pierced by the microneedle procedure and that the operation with the microneedle caused less damage to the retinal veins. Although it was possible to successfully pierce and inject vessels with 25% of the micropipettes used in this study, the structure of the retinal vessels at the sites where they were successfully pierced with the micropipettes was severely damaged.

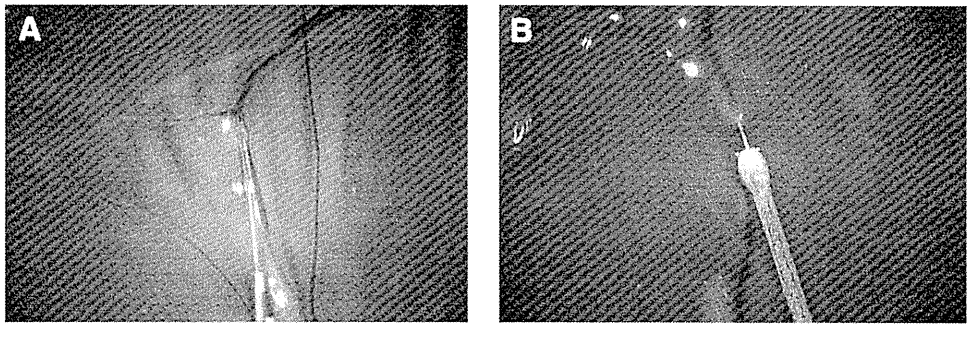

FIGURE 4. Retinal vein cannulation procedure in a porcine eye with a micropipette (A) and a microfabricated needle (B). A major retinal vein branch close to the optic nerve head was pierced with the micropipette or the microneedle. Retrograde blood flow was seen in both successful procedures (A and B).

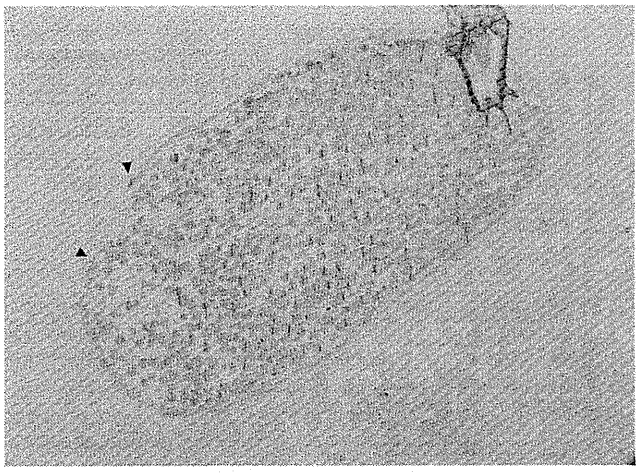

FIGURE 5. Photomicrograph of a cross-section of a retinal vein pierced with a microneedle in a porcine eye. The retinal vasculature is completely patent, and the laceration of the retinal vein wall is very clean (*arrowheads*). No preretinal hemorrhages are present.

There was a limitation in this study. The micropipettes used in this study are shown in Figures 1 and 2 and, unfortunately, were not the same as the micropipettes that Weiss and Bynoe used in their study.[5] If we had used the same micropipettes and compared the feasibility of the piercing procedure with the two instruments, the results would have been more reliable. Because the micropipettes used in this study were manufactured with a 30° beveled tip, they may be comparable to those used by other investigators.

The findings in this study may contribute to the development of the endovascular approach to the retinal vein. However, because fibrinolysis by injection of such drugs as the tissue plasminogen activator (t-PA) can be effective against central vein occlusion only in eyes with recently formed clots, the effectiveness of the tissue plasminogen activator injection of retinal veins is still unclear. Therefore, further investigation will be needed to ascertain the effectiveness of retinal endovascular surgery for eyes with retinal vein occlusion.

In conclusion, the feasibility of performing microvascular punctures and intravascular injections of retinal veins was demonstrated in porcine eyes. Solutions can be administered into the retinal vessels more effectively with a microfabricated needle, and that may contribute to improving the success of retinal endovascular surgery in human eyes.

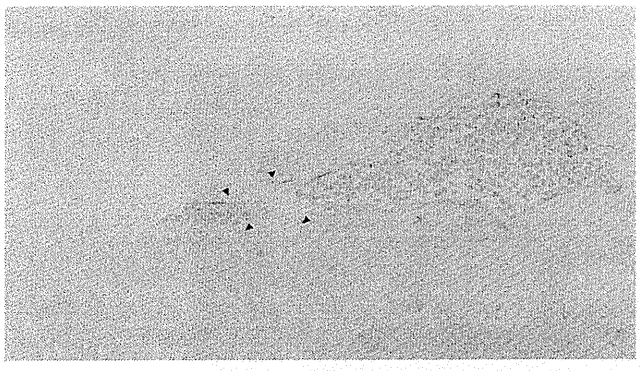

FIGURE 6. Photomicrograph of a cross-section of a retinal vein pierced with a micropipette in a porcine eye. The retinal vasculature is severely damaged, and the vessel is penetrated by the microneedle (*arrowheads*).

References

1. Green WR, Chan CC, Hutchins GM, Terry JM. Central retinal vein occlusion: a prospective histopathologic study of 29 eyes in 28 cases. *Trans Am Ophthalmol Soc.* 1981;79:371-422.
2. The central vein occlusion study group. Natural history and clinical management of central retinal vein occlusion. *Arch Ophtalmol.* 1997;115:486-491.
3. Allf BE, de Juan E Jr. In vivo cannulation of retinal vessels. *Graefes Arch Clin Exp Ophthalmol.* 1987;231:405-407.
4. Weiss JN. Treatment of central retinal vein occlusion by injection of tissue plasminogen activator into a retinal vein. *Am J Ophthalmol.* 1992;113:429-434.
5. Weiss JN, Bynoe LA. Injection of tissue plasminogen activator into a branch retinal vein in eyes with central retinal vein occlusion. *Ophthalmology.* 2001;108:2249-2257.
6. Glucksberg MR, Dunn R, Giebs CP. In vivo micropuncture of retinal vessels. *Graefes Arch Clin Exp Ophthalmol.* 1993;231:405-407.
7. Han SK, Kim SW, Kim WK. Microvascular anastomosis with minimal suture and fibrin glue: experimental and clinical study. *Microsurgery.* 1998;18:306-311.
8. Fekrat S, de Juan E. Chorioreinal venous anastomosis for central retinal vein occlusion: transvitreal venipuncture. *Ophthalmic Surg Lasers.* 1999;30:52-55.
9. Tang WM, Han DP. A study of surgical approaches to retinal vascular occlusions. *Arch Ophthalmol.* 2000;118:138-143.
10. Weiss J. Retinal surgery for treatment of central retinal occlusion. *Ophthalmic Surg Lasers.* 2000;31:162-165.
11. Suzuki Y, Matsuhashi H, Nakazawa M. In vivo retinal vascular cannulation in rabbits. *Graefes Arch Clin Exp Ophthalmol.* 2003; 241:585-588.
12. Tsillimbaris MK, Lit ES, D'Amico DJ. Retinal microvascular surgery: a feasibility study. *Invest Ophthalmol Vis Sci.* 2004;45:1963-1986.
13. Tameesh MK, Lakhanpal RR, Fujii GY, et al. Retinal vein cannulation with prolonged infusion of tissue plasminogen activator for the treatment of experimental retinal vein occlusion in dogs. *Am J Ophthalmol.* 2004;134:829-839.
14. Bynoe LA, Huchins RK, Lazarus HS, Friedberg MA. Retinal endovascular surgery for central retinal vein occlusion. *Retina.* 2005; 25:625-632.
15. Felgen N, Junker B, Agostini H, Hansen LL. Retinal endovascular lysis in ischemic central retinal vein occlusion. *Ophthalmology.* 2007;114:716-723.
16. Feltgen N, Agostini H, Auw-Haedrich C, Hansen L. Histopathologic findings after retinal endovascular lysis in central retinal vein occlusion. *Br J Ophthalmol.* 2007;91:558-559.
17. Yamamoto T, Kamei M, Sakaguchi H, et al. Comparison of surgical treatments for central retinal vein occlusion; RON vs. cannulation of tissue plasminogen into the retinal vein. *Retina.* 2009;29:1167-1174.
18. Moren H, Ungren P, Gesslein B, Olivecrona GK, Andreasson S, Malmsjo M. The porcine retinal vasculature accessed using an endovascular approach: a new experimental model for retinal ischemia. *Invest Ophthalmol Vis Sci.* 2009;50:5504-5510.
19. Yamamoto T, Kamei M, Sayanagi K, et al. Simultaneous intravitreal injection of triamcinolone acetonide and tissue plasminogen activator for central retinal vein occlusion: a pilot study. *Br J Ophthalmol.* 2011;95:69-73.
20. Wang WH, Kaskar K, Gill J, DeSplinter T. A simplified technique for embryo biopsy for preimplantation genetic diagnosis. *Fertil Steril.* 2008;90:438-442.
21. Kaushik S, Allen HH, Donald DD, et al. Lack of pain associated with microfabricated microneedles. *Anesth Analg.* 2001;92:502-504.
22. Prausnitz MR. Microneedles for transdermal drug delivery. *Adv Drug Deliv Rev.* 2004;56:581-587.
23. McAllister DV, Wang PM, Davis SP, et al. Microfabricated needles for transdermal delivery of macromolecules and nanoparticles: fabrication methods and transport studies. *Proc Natl Acad Sci U S A.* 2003;100:13755-13760.
24. Parks SS, Sigelman J, Gragoudas ES. The anatomy and cell biology of the retina. In: Tasman W, Jaeger EA, eds. *Duane's Foundations of Clinical Ophthalmology.* Vol. 1. Philadelphia: Lippincott Williams & Wilkins; 1999:21-50.

NUMBER 1 OF 1

AUTHOR QUERIES

DATE 11/1/2010
JOB NAME IAE

ARTICLE IAE201853
QUERIES FOR AUTHORS Sakamoto and Ishibashi

THIS QUERY FORM MUST BE RETURNED WITH ALL PROOFS FOR CORRECTIONS

AU1) Please provide city and the country names for the second affiliation.
AU2) Please note that the reference citation "Hogan" has been changed to "Hogan et al" as per the reference list. Please check if this is correct.
AU3) Please note that the reference citation "Haddad et al" has been changed to "Haddad and André" as per the reference list. Please check if this is correct.
AU4) Please provide the chapter title in reference 1.
AU5) For references 7, 11–14, 17, 23, 30–34, 36, 38, 41, 42, 44–46, 48, 49, 52, 53, and 55, if the total number of authors is 6 or fewer, please provide names of all the authors. If the number of authors is more than 6, then provide the names of first 3 authors followed by et al.
AU6) Please note that the arrow is not clearly shown in the artwork of "Figure 1B." Please check.
AU7) Please provide documentation for permission from the respective authors for using "Figures 1, 4, and 5." This documentation is needed before the publication can proceed.

Review

HYALOCYTES: ESSENTIAL CELLS OF VITREOUS CAVITY IN VITREORETINAL PATHOPHYSIOLOGY?

TAIJI SAKAMOTO, MD, PHD,* TATSURO ISHIBASHI, MD, PHD†

Purpose: To review the present understanding of hyalocytes.

Methods: A review of recent studies that investigated the roles of hyalocytes in the pathophysiology of vitreous cavity.

Results: Studies on immunocytochemistry and chimeric mice with green fluorescent protein transgenic mice show that hyalocytes belong to the monocyte/macrophage lineage and derive from bone marrow. The effects of hyalocytes on vitreous cavity environment can be divided into three categories: synthesis of extracellular matrix, regulation of the vitreous cavity immunology, and modulation of inflammation. In noninflamed eyes, vitreous cavity is an immune-privileged site that is maintained by a system called vitreous cavity–associated immune deviation, in which hyalocytes play the role of antigen-presenting cells. However, cultured hyalocytes proliferate in response to inflammatory molecules and secrete vascular endothelial growth factor and urokinase-type plasminogen activator. A collagen gel embedded with hyalocytes contracts over time, which is enhanced by transforming growth factor-β but is inhibited by Rho kinase inhibitor. These results suggest that hyalocytes can be an exacerbating factor in inflamed eyes. Clinically, hyalocytes are frequently found in the surgically removed specimens of epiretinal membrane or proliferative vitreoretinopathy.

Conclusion: Elucidating the properties of hyalocytes is important to understand the biology of vitreous cavity and to develop novel treatments for vitreoretinal diseases.

RETINA 0:1–7, 2010

Recently, a number of novel therapies have been emerging in clinical ophthalmology, especially for vitreoretinal diseases. They include a new type of pars plana vitrectomy, novel drugs such as ranibizumab and pegaptanib, and gene-mediated therapy. Of note is that these therapies often use the vitreous cavity as a therapeutic place or platform; thus, a more detailed knowledge of the environment of the vitreous cavity is required.

The vitreous cavity is composed mainly of collagen fibers, hyaluronan, and some cells.[1] It has been reported that there are groups of cells in the cortical or peripheral vitreous.[1–5] These cells, currently called hyalocytes, have a lobulated nucleus, cytoplasmic projections, and moderate numbers of mitochondria. Hyalocytes are located at an average distance of 50 mm from the inner surface of the retina and are concentrated anteriorly at the vitreous base and posteriorly in the vicinity of optic disk. According to previous publications,[6–8] hyalocytes were regarded as resting cells, and hyalocytes have been studied less

From the *Department of Ophthalmology, Kagoshima University Graduate School of Medical and Dental Science, Kagoshima, Japan; and †Department of Ophthalmology, Kyushu University.

AQ : 1

Supported in part by a grant from the Research Committee on Chorioretinal Degeneration and Optic Atrophy, Ministry of Health, Labor, and Welfare, and by a Grant-in-Aid for Scientific Research from the Ministry of Education, Science, and Culture of the Japanese government.

An extract from this manuscript was presented at the 26th meeting of the Club Jules Gonin, Cape Town, South Africa, October 2006, and the 27th meeting of the Club Jules Gonin, St Moritz, Switzerland, September 2008.

The authors report no conflicts of interest.

Reprint requests: Taiji Sakamoto, MD, PhD, Department of Ophthalmology, Kagoshima University Graduate School of Medical and Dental Science, Sakuragaoka 8-35-1, Kagoshima 890-8520, Japan; e-mail: tsakamot@m3.kufm.kagoshima-u.ac.jp

extensively in comparison with other intraocular cells, such as retinal pigment epithelial cells. However, recent studies[9–12] have shown that hyalocytes play a significant role in maintaining the vitreous body as a transparent and avascular system actively rather than passively. Hyalocytes have been found to be present in various aspects of pathophysiology, which involve epiretinal membrane (ERM) formation, diabetic macular edema, proliferative vitreoretinopathy, and others.[10,12–14] Therefore, we would like to review our present knowledge of hyalocytes to better understand vitreoretinal pathophysiology and to develop new treatments.

Origin, Morphology, and Turnover of Hyalocytes

Hyalocytes are variously described by light microscopy as being spindle-shaped, rounded, or even star-shaped cells. Their nuclei are lobulated, and the cytoplasm is characterized by the presence of many secretory granules and a well-developed Golgi apparatus[4,15] (Figure 1, A–D). They are mainly distributed close to the retina at the vitreous base and in the posterior hyaloid.[15] Morphologic studies demonstrate that hyalocytes belong to the monocyte/macrophage lineage.[4,7,17–19] However, Hogan et al[15] reported that hyalocytes differ from macrophages because of a paucity of lysosomes. Immunocytochemical analysis shows that hyalocytes express a monocyte/macrophage cell marker but not CD68, glial fibrillary acidic protein, cellular retinaldehyde-binding protein, and cytokeratin.[9,20–23] These results indicate that hyalocytes are derived from a monocyte/macrophage lineage but not from glial cells or retinal pigment epithelial cells. Furthermore, a study on rat hyalocytes revealed a positive reaction for ED2 but not for ED1, confirming that hyalocytes have characteristics of tissue macrophages.[16]

Recently, enhanced green fluorescent protein transgenic mice have been generated; the tissues of enhanced green fluorescent protein transgenic mice are green under excitation light. Using enhanced green fluorescent protein transgenic mice, cell movements can be tracked in an in vivo model. We created chimeric mice by transplanting bone marrow from enhanced green fluorescent protein transgenic mice into irradiated wild mice.[10,16] The results show that hyalocytes were green fluorescent protein negative directly after bone marrow transplantation in chimeric mice; however, the number of green fluorescent protein–positive hyalocytes increased over time. More than 60% of hyalocytes were replaced by green fluorescent protein–positive cells within 4 months, and 90% of hyalocytes were green fluorescent protein positive within 7 months after bone marrow transplantation (Figure 2). The levels of residual macrophages might not have been maintained by their proliferation but by being produced in bone marrow under a physiologic condition with a turnover time of several months.[16] However, van Meurs et al[24] showed the half-life of vitreous macrophage was 4.8 days by allowing vitreous macrophages to phagocytose ^{141}Cerium (γ-emitter)-labeled microspheres. It is difficult to conclude that these groups studied the same type of vitreous cells; however, there might be several different cell lineages within the so-called hyalocytes.

Conversely, Gloor[25] described that hyalocytes would be in an independent tissue layer, in which the cells are replaced by reproduction because the hyalocytes showed increased mitotic activity after photocoagulation. Haddad and André observed that ^{3}H-thymidine was detected in the hyalocytes of the cortical vitreous after ^{3}H-thymidine injection and concluded that hyalocytes renew themselves inside the eye.[26] It is not clear whether hyalocytes are composed of cells of different origins or those of the same origin at different developmental stages. Although more detailed studies are necessary to answer these questions, it is safe to say that most hyalocytes originate from bone marrow, at least under physiologic conditions.

Functions of Hyalocytes

The functional properties of hyalocytes can be divided into the following three categories: synthesis of extracellular matrix (ECM), modulator of immune reaction, and modulator of inflammation.

Synthesis of Extracellular Matrix

Because hyalocytes appear in the vitreous at an early embryonic stage, it is reasonable to assume that hyalocytes produce vitreous collagen. It has been reported that chick vitreous collagen is synthesized by the neural retina at early embryonic stages, whereas the major contribution derives from cells within the vitreous body later in the development.[27] Also, hyalocytes are reported to be responsible for the production of hyaluronic acid in calf and primate.[28,29] Recently, it has been further confirmed that production of hyaluronan is modulated by cytokines, such as transforming growth factor (TGF)-β or platelet-derived growth factor-BB using cultured hyalocytes.[30] It was also shown that cultured porcine hyalocytes produce glycosaminoglycans and ECM, which is modulated by basic fibroblast growth factor and

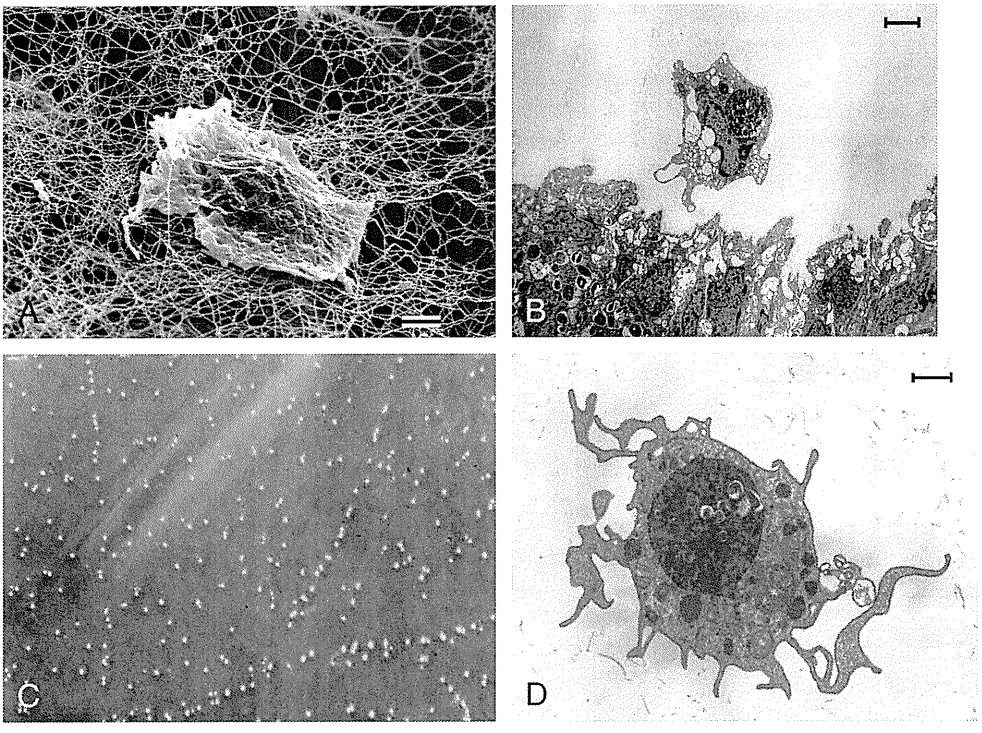

Fig. 1. Hyalocytes in animals. **A.** Scanning electron microscopic photograph of rat hyalocytes. Hyalocytes are present in collagen fibers. Bar 1 mm. **B.** Transmission electron microscopic photograph of rat hyalocytes. Hyalocytes are located close to the ciliary epithelium (arrow). Bar 1 mm. **C.** Phase-contrast microscopic photograph of bovine hyalocytes. Numerous hyalocytes are scattered in the vitreous (original magnification, ×10). **D.** Transmission electron microscopic photograph of bovine hyalocytes. Bar 1 mm. Reproduced with permission from Qiao et al,[16] Noda et al,[11] and Sakamoto.[10]

TGF-β1.[31] Because glycosaminoglycans are the stimulators of contraction of ECM with cells, the formation of a membrane with cells and ECM might be an important first step in the progression of ERM or proliferative vitreoretinopathy.[10,32] It is likely that hyalocytes play a certain role in this pathology by producing ECM in addition to other cells.[10,33–38]

Modulator of Intraocular Immune System: Vitreous Cavity–Associated Immune Deviation

The eye is an immune-privileged site that is styled to keep the visual pathway clear while at the same time to provide defenses against invading organisms.[39] Above all, the anterior chamber–associated immune deviation is a unique system to keep the eye immune privileged. Anterior chamber–associated immune deviation can be induced by antigen injection for peripheral tolerance to that antigen.[40] It is demonstrated that anterior chamber–associated immune deviation is induced by bone marrow–derived antigen-presenting cells, which are positive for F4/80, a marker of a wide range of mature tissue macrophages, localized in the iris and ciliary body in the eye and carrying an antigen-specific signal to the spleen.[39,41]

We investigated the mechanisms by which ocular inflammation associated with the vitreous cavity is reduced by injecting either ovalbumin or allogeneic splenocytes into the vitreous cavities of mice and assessed the effects of this on delayed-type hypersensitivity responses. After antigen inoculation into the vitreous cavity, antigen-specific delayed-type hypersensitivity responses were significantly impaired, and we named this phenomenon the vitreous cavity–associated immune deviation.[42] Vitreous cavity–associated immune deviation could also be induced by inoculating antigen-pulsed macrophages into the

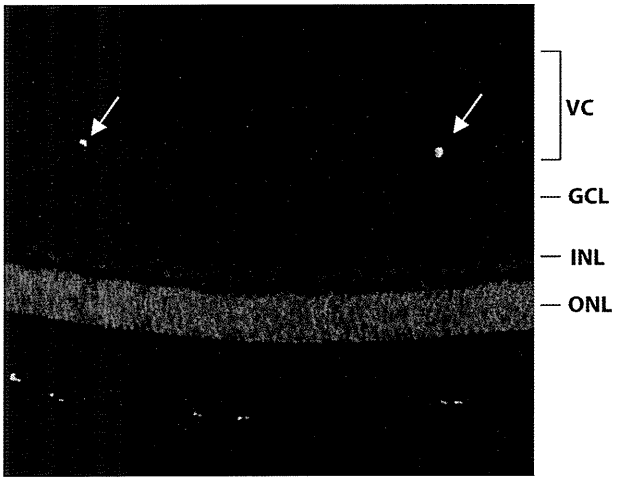

Fig. 2. Fluorescent microscopic photograph of GFP chimeric mouse. The hyalocytes (arrows) are GFP positive, indicating their bone marrow origin. VC, vitreous cortex; GCL, ganglion cell layer; INL, inner nuclear layer; ONL, outer nuclear layer; GFP, green fluorescent protein (original magnification, ×40).

COLOR

vitreous cavity. However, vitreous cavity–associated immune deviation did not develop either in mice with inflamed eyes, whether as a result of experimental autoimmune uveitis or coadministration of interleukin-6 in the vitreous cavity, or in knockout mice deficient in natural killer T cells.[42] In this system, we found that hyalocytes are the only cells present in the vitreous cavities. Interestingly, hyalocytes express F4/80, suggesting that hyalocytes are candidate antigen-presenting cells responsible for mediating vitreous cavity–associated immune deviation (Figure 3).[42] These findings suggest that hyalocytes would play a pivotal role in inhibiting intraocular inflammation in noninflamed eyes. F3

Modulator of Intraocular Inflammation

Almost three decades ago, human hyalocytes were reported to have characteristics of macrophages, such as phagocytic activity with surface receptors for IgG and complement components.[20] Macrophages are major cells in the inflammation of most tissues, so it is natural to assume that hyalocytes play a major role in intravitreous inflammation.

Cultured bovine hyalocytes proliferate in response to platelet-derived growth factor and secrete urokinase-type plasminogen activator (uPA).[11] Because uPA has a strong fibrinolytic activity by converting proenzyme plasminogen into serine protease plasmin, it might be beneficial to keep the vitreous cavity clear by removing fibrin and fibrin-related materials. At the same time, uPA is a multifunctional protein that also affects growth factor bioavailability; for example, uPA is a potent inducer of angiogenesis and tissue remodeling, so the role of uPA in ocular pathology would be complicated.[43] Similarly, cultured hyalocytes secrete VEGF, which is upregulated by hypoxia-inducible factor-1 or tumor necrosis factor-α.[44] Hyalocytes might be one of the cellular sources of intravitreous VEGF, which is a well-proven angiogenic and vascular permeability factor in diabetic retinopathy and exudative age-related macular degeneration.

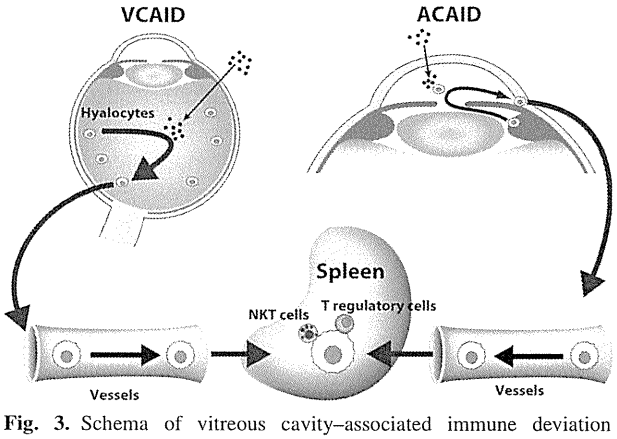

Fig. 3. Schema of vitreous cavity–associated immune deviation (VCAID) and anterior chamber–associated immune deviation (ACAID). Antigens inoculated into the vitreous cavity are captured by resident macrophage hyalocytes and carried via the bloodstream to the spleen. Both VCAID and ACAID require eye-derived antigen-presenting cells and CD1d-restricted natural killer T cells to induce antigen-specific regulatory T cells.

Recently, the role of hyalocytes in ocular pathology has been investigated from a different viewpoint. Contraction of the preretinal cortical vitreous is one of the most critical steps in various intraocular diseases. Three-dimensional collagen gel preparations have been used to assess the mechanism of membrane contraction in vitro, and this system is suitable for evaluating the cortical hyaloid contraction.[45] Using this system, the contractile property of hyalocytes was studied (Figure 4). As a result, a collagen gel embedded with hyalocytes contracts significantly in response to various stimulants, such as TGF-β2, and this effect is mediated through Rho and Rho kinase (ROCK)–dependent pathways.[46] This in vitro cell-mediated collagen gel contraction is more potent with hyalocytes than with retinal glial cells or retinal pigment epithelial cells.[10] Therefore, the presence of hyalocytes might be a potent exacerbating factor of preretinal membrane contraction in proliferative vitreoretinopathy after retinal detachment. F4

Clinical Implication

In histologic studies, several types of cell were found in preretinal membrane or posterior hyaloids, and macrophage-like cells were found frequently.[9,12,47–52] It is certain that some of them are hyalocytes (Figure 5). Kohno et al[33] found that cells located at the contractile epicenter of ERMs are mostly hyalocytes, not glial cells. Because hyalocytes have a strong contractile property, it may be assumed that hyalocytes play a critical role not only in the pathology of ERM but also in tractional retinal detachment.[32] Gandorfer et al[14] studied specimens of flat mount internal limiting membrane and found that macular hole formation is caused by the insertion of the cortical vitreous into the foveal internal limiting membrane and that cellular proliferation including hyalocytes is involved in vitreofoveal traction, resulting in a foveal tear. F5

To treat these pathologic conditions, removing ERM and posterior hyaloid is the preferred and logical approach at present because these membranes contain a number of cells including hyalocytes. The

COLOR

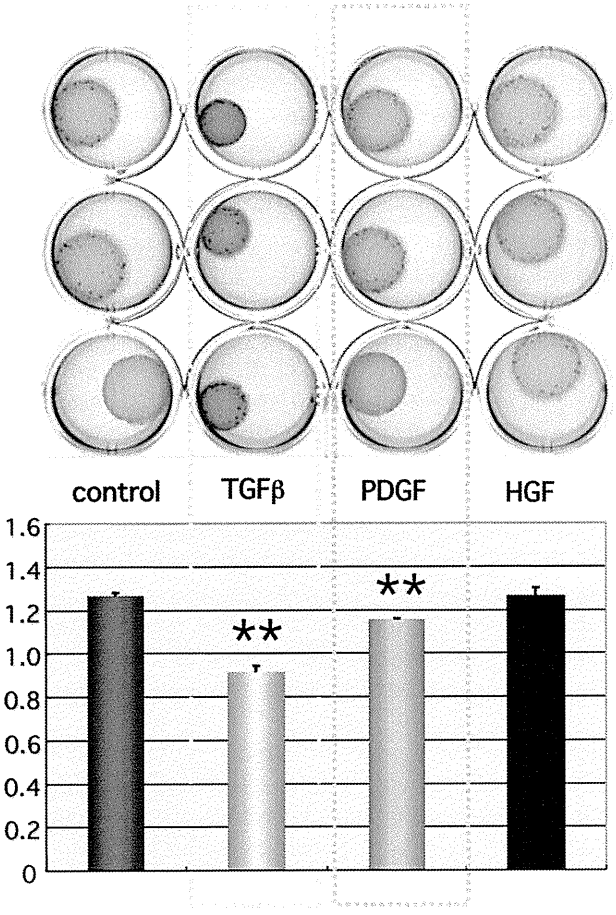

Fig. 4. Contraction of collagen gel embedded with hyalocytes. A collagen gel embedded with hyalocytes was stimulated with cytokines, such as TGF-β, platelet-derived growth factor (PDGF), or hepatocyte growth factor (HGF), and the size of the collagen gel was measured after 24 hours. The contraction of gel was significantly enhanced by TGF-β or PDGF (**$P < 0.01$). Reproduced with permission from Sakamoto.[10]

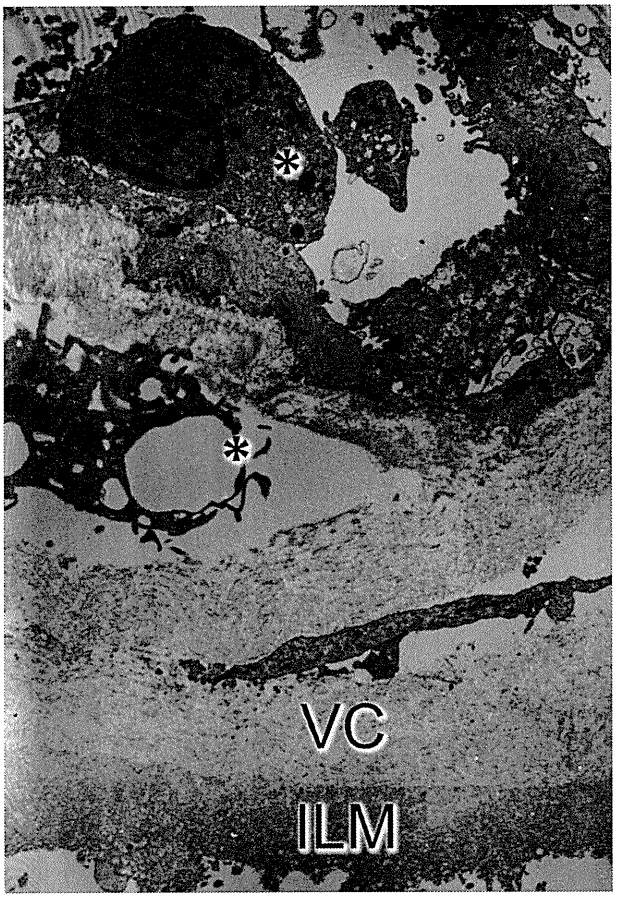

Fig. 5. Transmission electron microscopic photograph of surgically removed internal limiting membrane (ILM) from the eye of ERM. Macrophage-like cells (*) are present on the vitreous cortex (VC) and ILM. They are presumably hyalocytes. Reproduced with permission from Sakamoto[10] (original magnification, ×1800).

maneuver itself is not necessarily easy and recurrence is not rare. Adjunctive use of triamcinolone acetonide in vitrectomy is beneficial to remove these membranes securely and effectively.[53,54] Although this procedure is not always necessary in most of the cases, it might be beneficial for selected cases to reduce the incidence of postoperative preretinal fibrotic complications.[54] Complete removal of ERM together with internal limiting membrane resulted in a lower recurrence rate than incomplete removal, probably because the residual hyaloid or membrane becomes a scaffold of cell proliferation and ECM production by these cells.[55] If the residual hyaloid or internal limiting membrane is left alone without any cells, recurrence, namely reproduction of ECM by cellular elements after surgery, will not occur.

There are novel pharmacologic approaches to the disease. In an in vitro study, Rho and ROCK were found to play an important role in phosphorylation of the myosin light chain and the subsequent contraction; thus, a specific Rho kinase (ROCK) inhibitor fasudil could block contraction of collagen gel embedded with hyalocytes.[36] In rabbits, fasudil significantly inhibited the progression of experimental proliferative vitreoretinopathy without affecting the viability of retinal cells. ROCK, a key downstream mediator of TGF-β and other factors, might become a unique therapeutic target.[36] Of course, there is a distance between an animal study and the bedside; however, a pharmacologic approach to modulate hyalocytes might be a novel treatment of intraocular diseases.

Summary

As described above, there is no strict definition of "hyalocytes," but cells located at the periphery of vitreous cavity are called hyalocytes. The accumulating evidence shows that these hyalocytes can act as

COLOR

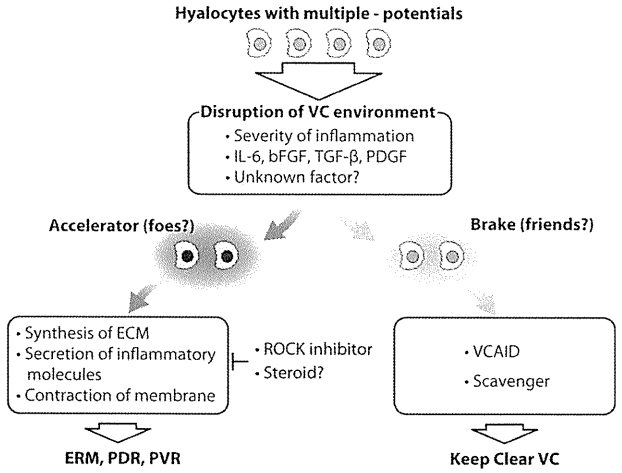

Fig. 6. Schema of possible roles of hyalocytes in ocular pathology. Hyalocytes are residual cells in vitreous cavity (VC) with multiple potentials. In the disruption of the VC environment, hyalocytes may act as an accelerator or a brake to destroy the clear vitreous dependent on unknown mechanisms. IL-6, interleukin-6; bFGF, basic fibroblast growth factor; PDGF, platelet-derived growth factor; PDR, proliferative diabetic retinopathy; PVR, proliferative vitreoretinopathy.

"friends" to keep the vitreous cavity clear by inhibiting immune reaction through vitreous cavity–associated immune deviation. At the same time, hyalocytes can act as "foes" by producing inflammatory cytokines and ECM followed by contraction of the membrane. Unfortunately, at present, it is difficult to tell what makes hyalocytes "friends" or "foes" (Figure 6). Further studies to answer this question might provide a key to a better understanding of microenvironment of the vitreous cavity and to developing an effective treatment for intraocular diseases.

F6

Key words: antigen-presenting cells, fibronectin, macular edema, VCAID, vitrectomy.

References

AQ : 4

1. Green WR, Seberg J. In: Ryan SJ, ed. Retina. 4th ed. St Louis, MO: Mosby; 2006:1921–1989.
2. Szirimai JA, Balazs EA. Studies on the structure of the vitreous body. III. Cells in the cortical layer. AMA Arch Ophthalmol 1958;59:34–48.
3. Hamburg A. Some investigations on the cells of the vitreous body. Ophthalmologica 1959;138:81–107.
4. Balazs EA, Toth LZJ, Eeckl EA, Mitchel AP. Studies on the structure of the vitreous body. XII. Cytological and histochemical studies on the cortical tissue layer. Exp Eye Res 1964; 3:57–71.
5. Sebag J. The vitreous. In: Hart WM Jr, ed. Adler's Physiology of the Eye. 9th ed. St Louis, MO: Mosby Year Book; 1992: 268–347.
6. Gloor BP. Development of the vitreous body and zonula. Graefes Arch Clin Exp Ophthalmol 1973;187:21–44.
7. Salu P, Claeskens W, De Wilde A, et al. Light and electron microscopic studies of the rat hyalocyte after perfusion fixation. Ophthalmic Res 1985;17:125–130. AQ : 5
8. Uehara M, Imagawa T, Kitagawa H. Morphological studies of the hyalocytes in the chicken eye: scanning electron microscopy and inflammatory response after the intravitreous injection of carbon particles. J Anat 1996;188:661–669.
9. Zhu M, Provis JM, Penfold PL. The human hyaloid system: cellular phenotypes and inter-relationships. Exp Eye Res 1999; 68:553–563.
10. Sakamoto T. Cell biology of hyalocytes. Nippon Ganka Gakkai Zasshi 2003;107:866–882.
11. Noda Y, Hata Y, Hisatomi T, et al. Functional properties of hyalocytes under PDGF-rich conditions. Invest Ophthalmol Vis Sci 2004;45:2107–2114.
12. Matsumoto H, Yamanaka I, Hisatomi T, et al. Triamcinolone acetonide-assisted pars plana vitrectomy improves residual posterior vitreous hyaloid removal: ultrastructural analysis of the inner limiting membrane. Retina 2007;27:174–179.
13. Ueno A, Enaida H, Hata Y, et al. Long-term clinical outcomes and therapeutic benefits of triamcinolone-assisted pars plana vitrectomy for proliferative vitreoretinopathy: a case study. Eur J Ophthalmol 2007;17:392–398.
14. Gandorfer A, Scheler R, Haritoglou C, et al. Pathology of the macular hole rim in flat-mounted internal limiting membrane specimens. Retina 2009;29:1097–1105.
15. Hogan MJ, Alvadadr JA, Weddel JE. Histology of the Human Eye. Philadelphia, PA: WB Sanders; 1971.
16. Qiao H, Hisatomi T, Sonoda KH, et al. The characterisation of hyalocytes: the origin, phenotype, and turnover. Br J Ophthalmol 2005;89:513–517.
17. Balazs EA, Toth LZ, Ozanics V. Cytological studies on the developing vitreous as related to the hyaloid vascular vessel system. Graefes Arch Clin Exp Ophthalmol 1980;213:71–85.
18. Saga T, Tagawa Y, Takeuchi T, et al. Electron microscopic study of cells in vitreous of guinea pig. Jpn J Ophthalmol 1984; 28:239–247.
19. Ogawa K. Scanning electron microscopic study of hyalocytes in the guinea pig eye. Arch Histol Cytol 2002;65:263–268.
20. Grabner G, Boltz G, Förster O. Macrophage-like properties of human hyalocytes. Invest Ophthalmol Vis Sci 1980;19: 333–340.
21. Jacobson B. Degradation of glycosaminoglycans by extracts of calf vitreous hyalocytes. Exp Eye Res 1984;39:373–385.
22. Lazarus HS, Hageman GS. In situ characterization of the human hyalocyte. Arch Ophthalmol 1994;112:1356–1362.
23. Schönfeld CL. Hyalocytes inhibit retinal pigment epithelium cell proliferation in vitro. Ger J Ophthalmol 1996;5: 224–228.
24. van Meurs JC, Sorgente N, Gauderman WJ, Ryan SJ. Clearance rate of macrophages from the vitreous in rabbits. Curr Eye Res 1990;9:683–686.
25. Gloor BP. Mitotic activity in the cortical vitreous cells (hyalocytes) after photocoagulation. Invest Ophthalmol 1969;8:633–646.
26. Haddad A, André JC. Hyalocyte-like cells are more numerous in the posterior chamber than they are in the vitreous of the rabbit eye. Exp Eye Res 1998;66:709–718.
27. Newsome DA, Linsenmayer TF, Trelstad RL. Vitreous body collagen. Evidence for a dual origin from the neural retina and hyalocytes. J Cell Biol 1976;71:59–67.
28. Osterlin SE, Jacobson B. The synthesis of hyaluronic acid in vitreous. I. Soluble and particulate transferases in hyalocytes. Exp Eye Res 1968;7:497–510.

29. Rittig M, Flügel C, Prehm P, Lütjen-Drecoll E. Hyaluronan synthase immunoreactivity in the anterior segment of the primate eye. Graefes Arch Clin Exp Ophthalmol 1993;231: 313–317.
30. Nishitsuka K, Kashiwagi Y, Tojo N, et al. Hyaluronan production regulation from porcine hyalocyte cell line by cytokines. Exp Eye Res 2007;85:539–545.
31. Sommer F, Pollinger K, Brandl F, et al. Hyalocyte proliferation and ECM accumulation modulated by bFGF and TGF-beta1. Graefes Arch Clin Exp Ophthalmol 2008;246:1275–1284.
32. Schaefer T, Roux M, Stuhlsatz HW, et al. Glycosaminoglycans modulate cell-matrix interactions of human fibroblasts and endothelial cells in vitro. J Cell Sci 1996;109:479–488.
33. Kohno RI, Hata Y, Kawahara S, et al. Possible contribution of hyalocytes to idiopathic epiretinal membrane formation and its contraction. Br J Ophthalmol 2009;93:1020–1026.
34. Kita T, Hata Y, Kano K, et al. Transforming growth factor-beta2 and connective tissue growth factor in proliferative vitreoretinal diseases: possible involvement of hyalocytes and therapeutic potential of Rho kinase inhibitor. Diabetes 2007; 56:231–238.
35. Kampik A, Green WR, Michels RG, Nase PK. Ultrastructural features of progressive idiopathic epiretinal membrane removed by vitreous surgery. Am J Ophthalmol 1980;90: 797–809.
36. Kita T, Hata Y, Arita R, et al. Role of TGF-beta in proliferative vitreoretinal diseases and ROCK as a therapeutic target. Proc Natl Acad Sci U S A 2008;105:17504–17509.
37. Sebag J. Anomalous posterior vitreous detachment: a unifying concept in vitreo-retinal disease. Graefes Arch Clin Exp Ophthalmol 2004;242:690–698.
38. Sebag J, Gupta P, Rosen RR, et al. Macular holes and macular pucker: the role of vitreoschisis as imaged by optical coherence tomography/scanning laser ophthalmoscopy. Trans Am Ophthalmol Soc 2007;105:121–129.
39. Stein-Streilein J. Immune regulation and the eye. Trends Immunol 2008;29:548–554.
40. Streilein JW. Ocular immune privilege: therapeutic opportunities from an experiment of nature. Nat Rev Immunol 2003;3: 878–889.
41. Streilein JW, Okamoto S, Hara Y, et al. Blood-borne signals that induce anterior chamber-associated immune deviation after intracameral injection of antigen. Invest Ophthalmol Vis Sci 1997;38:2245–2254.
42. Sonoda KH, Sakamoto T, Qiao H, et al. The analysis of systemic tolerance elicited by antigen inoculation into the vitreous cavity: vitreous cavity-associated immune deviation. Immunology 2005;116:390–399.
43. Tkachuk VA, Plekhanova OS, Parfyonova YV. Regulation of arterial remodeling and angiogenesis by urokinase-type plasminogen activator. Can J Physiol Pharmacol 2009;87: 231–251.
44. Hata Y, Sassa Y, Kita T, et al. Vascular endothelial growth factor expression by hyalocytes and its regulation by glucocorticoid. Br J Ophthalmol 2008;92:1540–1544.
45. Sakamoto T, Hinton DR, Sakamoto H, et al. Collagen gel contraction induced by retinal pigment epithelial cells and choroidal fibroblasts involves the protein kinase C pathway. Curr Eye Res 1994;13:451–459.
46. Hirayama K, Hata Y, Noda Y, et al. The involvement of the rho-kinase pathway and its regulation in cytokine-induced collagen gel contraction by hyalocytes. Invest Ophthalmol Vis Sci 2004; 45:3896–3903.
47. Wiedemann P, Kohlmann H. Perioperative analysis of vitreous cell components by immunoimpression cytology. Graefes Arch Clin Exp Ophthalmol 1996;123:463–466.
48. Gandorfer A, Rohleder M, Grosselfinger S, et al. Epiretinal pathology of diffuse diabetic macular edema associated with vitreomacular traction. Am J Ophthalmol 2005;139: 638–652.
49. Kampik A, Kenyon KR, Michels RG, et al. Epiretinal and vitreous membranes: comparative study of 56 cases. Arch Ophthalmol 1981;99:1445–1454.
50. Faulborn J, Dunker S, Bowald S. Diabetic vitreopathy: findings using the celloidin embedding technique. Ophthalmologica 1998;212:369–376.
51. Kishi S, Numaga T, Yamazaki, S. Structure of the inner retinal surface in simple diabetic retinopathy. Jpn J Ophthalmol 1982; 26:141–149.
52. Hisatomi T, Enaida H, Sakamoto T, et al. A new method for comprehensive bird's-eye analysis of the surgically excised internal limiting membrane. Am J Ophthalmol 2005;139: 1121–1122.
53. Enaida H, Hata Y, Ueno A, et al. Possible benefits of triamcinolone-assisted pars plana vitrectomy for retinal diseases. Retina 2003;23:764–770.
54. Sakamoto T, Ishibashi T. Visualizing vitreous in vitrectomy by triamcinolone. Graefes Arch Clin Exp Ophthalmol 2009;247: 1153–1163.
55. Shimada H, Nakashizuka H, Hattori T, et al. Double staining with brilliant blue G and double peeling for epiretinal membranes. Ophthalmology 2009;116:1370–1376.

Laboratory Investigation (2011), 1–14

NSAIDs inhibit neovascularization of choroid through HO-1-dependent pathway

Narimasa Yoshinaga[1], Noboru Arimura[1], Hiroki Otsuka[1], Ko-ichi Kawahara[2], Teruto Hashiguchi[2], Ikuro Maruyama[3] and Taiji Sakamoto[1]

Intraocular neovascularization is the leading cause of severe visual loss and anti-vascular endothelial growth factor (VEGF) therapy is currently performed for choroidal neovascularization (CNV). Despite its potent anti-angiogenic effect, there are concerns about its long-term safety. Non-steroidal anti-inflammatory drugs (NSAIDs) are common therapeutic agents used for treating inflammatory diseases, and their anti-stress effects are attracting attention now. We studied the effects of topical NSAIDs on CNV, focusing on anti-stress proteins. Cultured retinal pigment epithelium (RPE) cells were treated with NSAIDs: bromfenac, indomethacin, or vehicle control. Transcription factor NF-E2-related factor 2 (Nrf2) and its downstream anti-oxidant protein heme oxygenase (HO)-1 were assessed using western blot and immunohistochemistry. As a result, NSAIDs induced translocation of Nrf2 into the nucleus and the robust expression of HO-1 in a dose- and time-dependent manner. Flow cytometric analysis revealed that bromfenac inhibited H_2O_2-induced apoptosis in cultured RPE cells. Next, we studied the effects of topical bromfenac on laser-induced CNV model in rat. The expressions of Nrf2 and HO-1, infiltrations of ED-1-positive macrophages at CNV lesions and size were analyzed. VEGF in the ocular fluid of these rats was also measured using enzyme-linked immunosorbent assay. Rats administered an inhibitor of HO-1 stannic mesoporphyrin (SnMP) were also studied. The results showed that topical bromfenac led to translocation of Nrf2 and induction of HO-1 in CNV lesions and that the number of infiltrating macrophages at the CNV lesion decreased. The sizes of CNV lesions were significantly smaller in bromfenac-treated rats than control CNV, and the effects were diminished by SnMP. VEGF increased in the ocular fluid after laser treatment and was inhibited by bromfenac and SnMP canceling these effects. NSAIDs inhibit CNV through the novel anti-stress protein HO-1-dependent pathway, indicating its potential therapeutic value for various intraocular angiogenic diseases including CNV.

Laboratory Investigation (2011) **0,** 000–000. doi:10.1038/labinvest.2011.101

KEYWORDS: age-related macular degeneration; anti-VEGF; choroidal atrophy; photodynamic therapy; oxidative stress; steroid

Ocular angiogenesis such as choroidal neovascularization (CNV) is a leading cause of severe vision loss in patients with various ocular diseases.[1–3] Until recently, CNV was not a treatable condition and visual prognosis was poor. However, novel pharmacological therapies such as anti-vascular endothelial growth factor (VEGF) have revolutionized this field.[4,5] Despite significant advances, there are still concerns about the present anti-VEGF treatment. Complete blocking of VEGF is a logically correct method; however, it may induce retinal damage after a long period, because VEGF is a neurotrophic factor and has an important role in the retinal development and neuroprotection.[6,7] There are several reports showing that complete blocking of VEGF results in retinal degeneration in animals.[8,9] Indeed, unexplainable retinal atrophy was noted in some eyes with age-related macular degeneration (AMD) treated after several years of intense anti-VEGF therapy.[10]

Recently, it was reported that non-steroidal anti-inflammatory drugs (NSAIDs) inhibit CNV in animals and a large retrospective study found a reduced incidence of CNV in AMD patients taking aspirin.[11–17] The anti-inflammatory properties of NSAIDs are believed to reside in their ability to inhibit the activity of cyclooxygenase (COX). Indeed COX2 was shown to have a pivotal role in the expression of VEGF in

[1]Department of Ophthalmology, Kagoshima University Graduate School of Medical and Dental Sciences, Kagoshima, Japan; [2]Department of Laboratory and Vascular Medicine, Kagoshima University Graduate School of Medical and Dental Sciences, Kagoshima, Japan and [3]Department of Systems Biology in Thromboregulation, Kagoshima University Graduate School of Medical and Dental Sciences, Kagoshima, Japan
Correspondence: Professor T Sakamoto, MD, PhD, Department of Ophthalmology, Kagoshima University Graduate School of Medical and Dental Sciences, 8-27-1, Sakuragaoka, Kagoshima 890-8520, Japan.
E-mail: tsakamot@m3.kufm.kagoshima-u.ac.jp

Received 17 January 2011; revised 30 March 2011; accepted 28 April 2011

a CNV animal model.[18] However, NSAIDs have other biological actions that inhibit nuclear factor-κB (NF-κB), which has a central role in the expression of various pro-inflammatory mediators.[19] Nonetheless, the real mechanism whereby NSAIDs inhibit CNV is not fully understood.

Heme oxygenase-1 (HO-1) is an anti-stress protein. Not only its substrate, heme, but also various stressors such as oxidative stressors, ultraviolet irradiation, inflammatory cytokines, and heavy metals have been reported to induce HO-1 production.[20–22] HO-1 degrades heme to carbon monoxide (CO), free iron, and biliverdin. Biliverdin is subsequently converted into bilirubin by biliverdin reductase.[20–22] Bilirubin and biliverdin are potent antioxidants, and CO has an anti-apoptotic activity. Therefore, upregulation of HO-1 in cells makes the cells resistant to apoptosis induced by various stressors. It was recently reported that NSAIDs upregulate HO-1 production in some types of cell.[23–27] If this anti-stress effect were inducible with topical NSAIDs, it would be very beneficial to use NSAIDs for the treatment of angiogenesis, because they may inhibit both pathological angiogenesis and potential collateral damage related to treatment. This would be especially advantageous for angiogenic disorders of the central nervous system including CNV. In this study, we explore the influence of NSAIDs on the regulation of anti-stress proteins *in vitro* focusing on their anti-apoptotic action and further on their effects on CNV models *in vivo*.

MATERIALS AND METHODS

Cell Culture

All experiments *in vitro* were performed using ARPE-19, a human diploid retinal pigment epithelium (RPE) cell line, which is in many ways similar to RPE *in vivo* (American Type Culture Collections, Manassas, VA).[28] All cultures were fed twice weekly with Dulbecco's modified Eagle's medium: nutrient mixture F12, plus 10% (vol/vol) fetal bovine serum, 2 mM L-glutamine, and penicillin–streptomycin at 100 IU/ml. Cultures were incubated at 37 °C in 5% (vol/vol) CO_2 incubator and sub-cultured with 0.05% trypsin–EDTA (all products were obtained from Invitrogen-Gibco, Rockville, MD). Subconfluent cultures were trypsinized and seeded for the following experiments.

Western Blot Analysis of NF-E2-Related Factor 2 (Nrf2) and HO-1

ARPE-19 cells were subcultured on 6-cm tissue culture dishes. The cells were serum starved for 3 h and stimulated with the indicated concentration of indomethacine (Funakoshi, Tokyo, Japan), bromfenac (provided from Senju Pharmaceutical, Osaka, Japan) as NSAIDs, or dimethylsulfoxide (DMSO) as control for the indicated time. Nuclear and cytoplasmic extracts of cells were prepared using the Pierce NE-PER nuclear and cytoplasmic extraction kit (Pierce, Rockford, IL). They were subjected to 10% SDS–polyacrylamide gel electrophoresis and transferred to nitrocellulose membranes (GE Healthcare Bio-sciences KK, Piscataway, NJ) as with our previous methods.[28,29] Membranes were incubated with a blocking buffer containing 1% BSA and 5% non-fat milk in 25 mM Tris–HCl-buffered saline with 0.02% Tween 20 (TBST), followed by incubation with the respective primary antibodies (1:200; anti-Nrf2 rabbit polyclonal antibody, 1:500; anti-HO-1 antibody, 1:200; anti-β-actin goat polyclonal antibody, Santa Cruz Biotechnology Inc., CA) in TBST containing 1% non-fat milk overnight at 4°C. After three washes with TBST, membranes were incubated with horseradish peroxidase (HRP)-conjugated anti-rabbit IgG polyclonal antibody (Santa Cruz Biotechnology Inc.) or HRP-conjugated anti-goat IgG polyclonal antibody diluted 1:3000 in TBST containing 2.5% non-fat milk for 1 h. The membrane was washed twice, and immunoreactive bands were visualized using an ECL detection system (GE Healthcare Bio-sciences KK). Immunoreactive bands were quantified and relative sum intensities of bands were compared using Image J Software (US National Institutes of Health).

Immunocytochemistry of Nrf2 and HO-1

Immunocytochemistry was carried out in accordance with our previous method.[28,29] ARPE-19 cells were grown on culture slides and serum starved for 3 h, then treated with the indicated concentration of indomethacin, bromfenac, or DMSO as the control for 3 h. After treatment, slides were washed with PBS, fixed with OptiLyse C (Beckman Coulter, Miami, FL), blocked with 1% BSA in PBS containing 0.1% of triton-X100 (PBST) for 60 min and incubated with polyclonal rabbit anti-Nrf2 and anti-HO-1 antibody (each 1:100; Santa Cruz Biotechnology Inc.) in PBS containing 1.5% BSA for 60 min at room temperature. The slides were washed with PBST, incubated with secondary antibodies, Alexa-Fluor 488-conjugated goat anti-mouse IgG F(ab)2 fragment, and Alexa-Fluor 594-conjugated goat anti-rabbit IgG F(ab)2 fragment (each 1:400; Molecular Probes, Carlsbad, CA) for an additional 60 min in the dark at room temperature. Stained cells were washed, mounted with Shandon Perma-Flour (Thermo Scientific, Waltham, MA), and examined with a Zeiss fluorescence microscope (Zeiss, Oberkochen, Germany).

Flow Cytometric Analysis

To analyze the cellular DNA content, the propidium iodide staining method was used as previously described. Briefly, ARPE-19 cells subcultured on 6-cm dishes at a density of 4.5×10^5 cells per dish and incubated with bromfenac or DMSO as a control were dissolved in medium with 1% fetal bovine serum for 24 h. After treatment for the indicated periods, the cells were washed with PBS. The pellet was resuspended in 70% ethanol (2 ml), and the suspension was incubated at −20 °C for 20 min. Cells were then incubated in the dark for 15 min with propidium iodide (5 g/ml) in PBS in the presence of RNase (5 g/ml). Then, the DNA content was

determined (2×10^4 cells each time) with a FACS analyzer (Epics; Beckman Coulter).

Cell Viability Assay

Cell viability was analyzed from mitochondrial respiratory activity measured using MTT (3-(4,5-dimethylthiazol-2yl)-2,5-diphenol tetrazolium bromide) assay (Wako Chemicals, Osaka, Japan), as described previously.[28] Briefly, 3.5×10^4 ARPE-19 cells were cultured in 24-well plates (500 ml medium per well) and pretreated with 2.5 μM bromfenac or DMSO dissolved in a medium with 1% fetal bovine serum for 24 h. Then, the cells were stimulated with or without hydrogen peroxide (500 μM; Merck, Darmstadt) for 15 min and incubated with MTT (0.5 mg/ml; final concentration) for 3 h. Formazan product was solubilized by the addition of DMSO for 16 h. Dehydrogenase activity was expressed as absorbance at a test wavelength of 570 nm and at a reference wavelength of 630 nm. Assays were performed in triplicate and repeated three times in independent experiments.

Animals

Brown-Norway rats (7 week old male; weight 140–160 g) were purchased from Kyudo (Fukuoka, Japan), and housed in a temperature-controlled room. The animals were kept on a 12-h light–dark schedule and had free access to food and water. All animals were treated in accordance with the ARVO Statement for the Use of Animals in Ophthalmic and Vision Research.

Induction of Experimental CNV

A rat CNV model was made accordance to our previous methods.[30,31] Briefly, rats were anesthetized with a 0.1–0.2 ml of a mixture of 100 mg/ml ketamine and 20 mg/ml xylazine. Pupils were dilated with a topical application of 5.0% phenylephrine and 0.8% tropicamide. CNV was experimentally produced with an argon dye-pulsed laser (Novus Varia, Lumenis, Salt Lake City, UT) and a slit lamp delivery system (SL-130; Carl Zeiss Meditec GmbH, Oberkochen, Germany) at a spot size of 100 μm, duration of 0.05 s, and intensity of 200 mW. Four laser photocoagulations were applied to each eye between the major retinal vessels around the optic disk under the previously described conditions.[30] The morphological end point of the laser injury was the appearance of a cavitation bubble, a sign that is thought to correlate with the disruption of Bruch's membrane. On occasion, the inducing laser burst created an extensive subretinal hemorrhage, and these spots were excluded from any further treatment or analysis.

Evaluation of Effects of Topical Bromfenac on Experimental CNV

A total of 20 male Brown-Norway rats were divided into saline-treated group and bromfenac-treated group. All rats underwent laser photocoagulation of the right eye as described above. Saline-treated group rats received eye drops of saline six times a day for 7 days. Drug administration was started the day after photocoagulation (day 1), and continued until day 7. Bromfenac-treated rats were received eye drops of human use bromfenac ophthalmic solution (Bronuk 0.1% ophthalmic solution, Senju Pharmaceutical) six times a day, for 7 days. The eyes were enucleated on day 8 and subjected to further examinations.

Choroidal Flat Mounts

Rats were anesthetized and perfused with 1 ml PBS containing 50 mg/ml fluorescein-labeled dextran (Sigma Aldrich, St Louis, MO) as previously described elsewhere.[12,13] After the eyes were enucleated and briefly fixed in 4% PFA, the anterior segment was removed and the retina was carefully dissected from the eyecup. Four to six radial cuts were made from the edge to the equator, and the eyecup was flat mounted with the sclera facing down and viewed with a Zeiss fluorescence microscope. Images were captured using the same exposure time for each comparative section, taken with a CCD camera, and the sizes of CNV lesions were measured using Image J.

Western Blot Analysis

Retina–choroid whole mounts were isolated and frozen at −80 °C within 2 min after enucleation. Retina–choroids were later ultrasonically homogenized and cytoplasmic protein extracts were isolated using a Pierce NE-PER nuclear and cytoplasmic extraction kit (Pierce) at 4 °C. The protein extracts (20 μg of protein in each lane) were subjected to the western blot analysis described above. For quantification, blots of five independent experiments were used.

Immunofluorescent Staining

Indirect immunofluorescent staining was carried out as described previously.[28,29] Enucleated eyes from the rats were immediately fixed in 4% paraformaldehyde at 4 °C for 12 h. The anterior segment and the lens were removed, and the remaining eyecup was cytoprotected with 10–30% sucrose in PBS. The eyecups were then frozen in an optimal cutting temperature compound (Sakura Finetech, Tokyo, Japan). Frozen sections (7 μm) were dried and blocked with blocking buffer for 1 h. The antibodies used for staining were rabbit polyclonal anti-Nrf2 antibody, rabbit polyclonal anti-HO-1 antibody (each 1:100; Santa Cruz Biotechnology Inc.), mouse anti-CD68 monoclonal antibody (ED1; 1:800; Serotec, Raleigh, NC), mouse anti-glial fibrillary acidic protein (GFAP) monoclonal antibody (1:400; Sigma Aldrich), mouse anti-RPE 65 monoclonal antibody, and mouse anti-CD31 monoclonal antibody (PECAM-1; 1:250 and 1:100, respectively; Abcam, Cambridge, UK). Normal rabbit or mouse IgG was used instead of primary antibody as a negative control in each case. Secondary antibodies were Alexa-Fluor 488-conjugated goat anti-mouse IgG F(ab)2 fragment and Alexa-Fluor 594-conjugated goat anti-rabbit IgG F(ab)2 fragment (each 1:400; Molecular Probes). Slides were

counterstained with DAPI, mounted with Shandon Perma-Fluor (Thermo Scientific), and viewed with a Zeiss fluorescence microscope. Images were captured using the same exposure time for each comparative section. For all experiments, at least three sections from each eye were evaluated. To quantify the macrophage infiltration, 10 different images were randomly selected by a controller (NY) and examined by masked observers (NA and HO).

Evaluation of Intraocular VEGF

We also measured concentrations of VEGF in the intraocular fluid (mixture of aqueous humor and vitreous fluid) as described previously with some modifications.[30] On day 8, the eyes were enucleated under deep anesthesia, the conjunctival tissue was removed, and the remaining eye tissues (cornea, iris, vitreous body, retina, choroids, and sclera) were collected in a tube and four to six radial cuts were made from the equator to cornea edge and to optic nerve at 4 °C. After centrifugation at 12 000 *g* for 30 s, supernatants were collected, and the concentrations of VEGF were measured using ELISA development kits (R&D Systems, Minneapolis, MN). VEGF concentration was adjusted by each protein concentration as previously described.[29] The adjusted concentration from a single eye was used as the concentration of VEGF.

Statistical Analysis

Because of the skewed distribution, the results were analyzed statistically using nonparametric tests (Mann–Whitney *U*-test) and were expressed as mean and range.

Statistical analyses were performed using SPSS software version 16.0 (SPSS Inc., Chicago, IL). A *P*-value of 0.05 was considered to be statistically significant. To adjust for inflated error resulting from multiple comparisons, the corrected significant *P*-value was defined as 0.05/4 using the Bonferroni correction for multiple comparisons.

RESULTS

NSAIDs Translocated Nrf2 and Upregulated HO-1 in Cultured RPE Cells

First, we examined whether transcriptional factor Nrf2 and phase 2 anti-oxidative protein HO-1 were expressed in ARPE-19 cells. Immunocytochemistry showed Nrf2 was located mainly in the cytoplasm and that HO-1 expression was barely detected in an untreated condition. After treatment with indomethacine or bromfenac, Nrf2 was translocated into the nucleus and HO-1 was abundantly present in the perinuclear lesion and cytoplasm (Figure 1).

Western blot analysis showed that treatment with indomethacine resulted in maximal immunoreactivity against Nrf2 at a concentration of 250 μM and 24 h of treatment, whereas HO-1 showed maximal band at a concentration of 50 μM, and this remained constant at 50–250 μM and showed maximal at 12 h of treatment. Treatment with bromfenac also showed maximal immunoreactivity for Nrf2 at a concentration of 160 μM. HO-1 showed maximal band at 40 μM and remained at 80 μM. Time-course examination showed maximal immunoreactivity at 12 h (Figure 2).

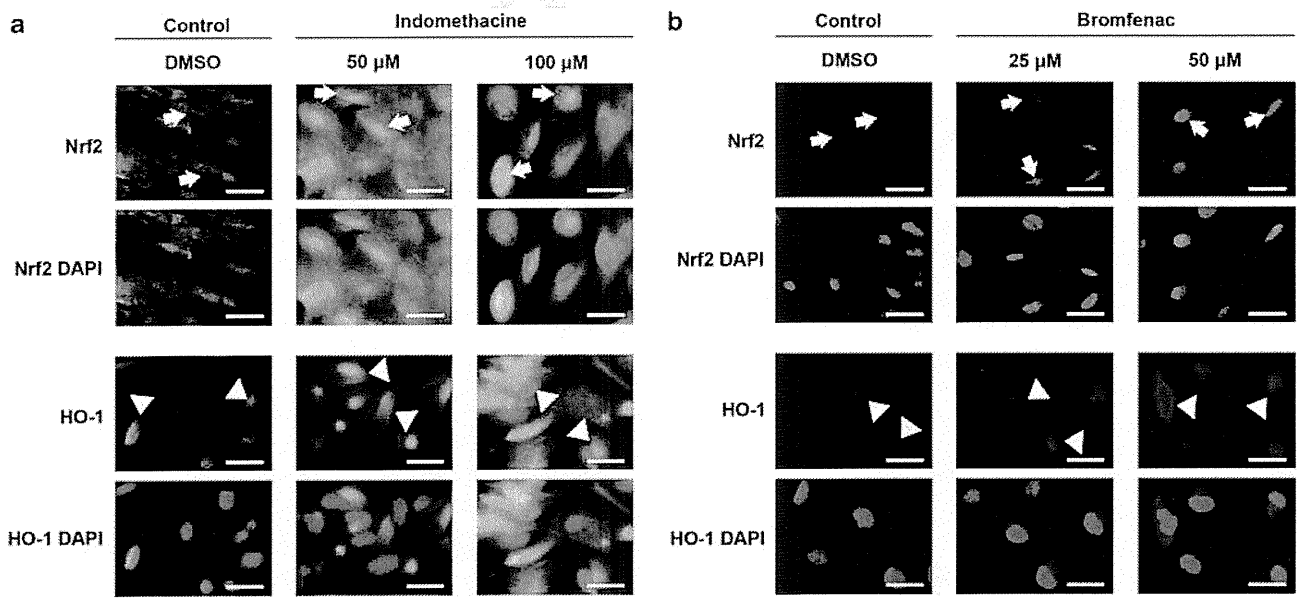

Figure 1 Expressions of Nrf2 and HO-1 protein in immunocytochemistry of ARPE-19 cells. (**a**) Treatment with the indicated concentration of indomethacine upregulated nuclear translocation of Nrf2. Nucleus was translucent or unstained in the control. On the other hand, Nrf2 was upregulated and nucleus is stained after indomethacine treatment (arrows). Cellular expressions of HO-1 were also upregulated in cytosol and nucleus (arrowheads). Scale bars: 30 μm. (**b**) Treatment with bromfenac also showed activation and increased Nrf2 expression in nucleus (arrows). Treatment with bromfenac increased the expression of HO-1 in nucleus and cytosol, especially around nucleus (arrowheads). Scale bars: 30 μm.

Bromfenac Inhibited RPE Cell Apoptosis Caused by Oxidative Stress

It has been reported that HO-1 has an anti-apoptotic property in human gastric mucosal cells.[32] We examined whether HO-1 induced by NSAIDs has functional properties against oxidative stress in ARPE-19 cells. H_2O_2 increased cell apoptosis in either DMSO-treated or bromfenac-treated cells ($15.6 \pm 4.01\%$ to $26.2 \pm 4.22\%$ in DMSO-treated control cells; $P<0.001$ *vs* $15.3 \pm 2.91\%$ to $20.3 \pm 3.02\%$ in bromfenac-treated cells; $P<0.005$). Apoptosis induced by oxidative stress was significantly less in bromfenac-treated cells compared with DMSO-treated control cells ($20.3 \pm 3.02\%$ bromfenac-treated cells *vs* $26.1 \pm 4.22\%$ DMSO-treated cells; $P<0.01$). Treatment with bromfenac itself resulted in no significant difference in apoptosis ($15.6 \pm 4.01\%$ DMSO-treated cells *vs* $15.3 \pm 2.91\%$ bromfenac-treated cells; $P=0.86$; Figure 3a and b).

We also tested cell viability in ARPE-19 cells using MTT assay. As described using propidium iodide staining and a FACS analyzer, H_2O_2 increased cell death of either DMSO-treated or bromfenac-treated cells (0% to $29.0 \pm 2.89\%$ in DMSO-treated control cells; $P<0.001$ *vs* $0.702 \pm 5.73\%$ to $23.5 \pm 4.04\%$ in bromfenac-treated cells; $P<0.001$). Cell death induced by oxidative stress was significantly less in bromfenac-treated cells compared with DMSO-treated control cells ($23.5 \pm 4.04\%$ bromfenac-treated cells *vs* $29.0 \pm 2.89\%$ DMSO-treated cells; $P<0.001$). Treatment with bromfenac itself made no significant difference to cell viability reduction (0% DMSO-treated cells *vs* $0.702 \pm 5.73\%$ bromfenac-treated cells; $P=0.519$;

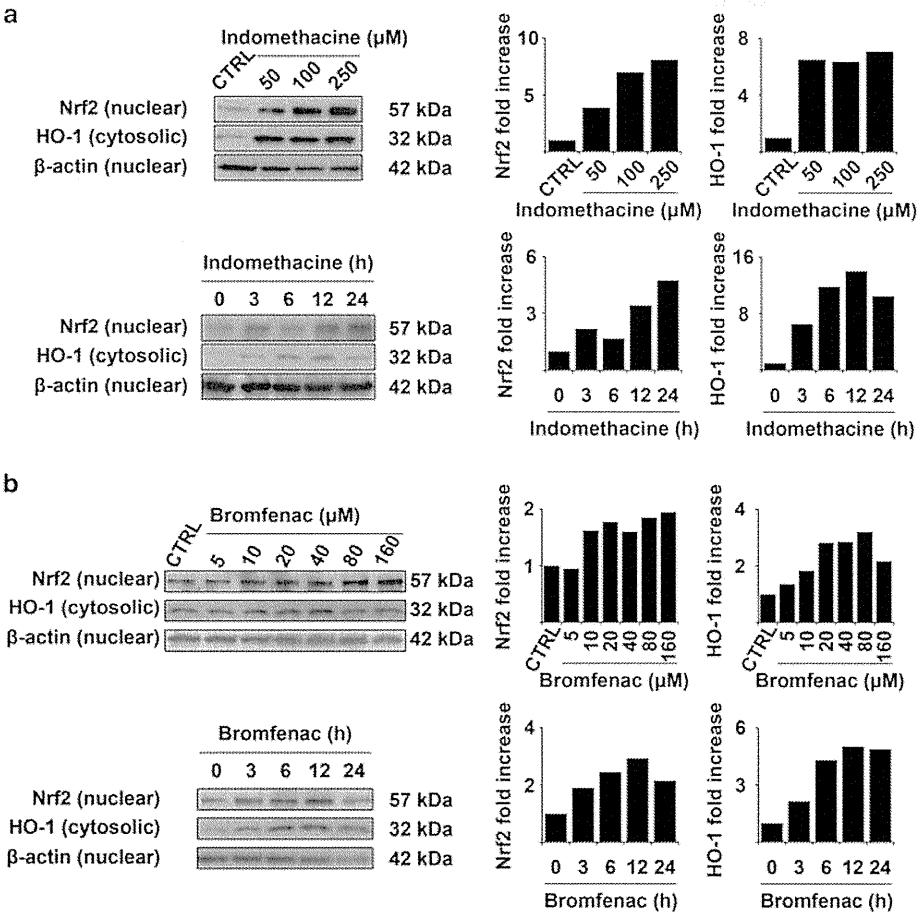

Figure 2 Nrf2 or HO-1 expression in ARPE19 cells by western blot analysis. (**a**; Top row) Serum-starved ARPE-19 cells were stimulated with indomethacine for 3 h and Nrf2 in nuclear protein and HO-1 in cytosolic protein were analyzed using western blots. Nrf2 in nuclear protein was increased by indomethacine in a dose-dependent manner. HO-1 in cytosolic protein is upregulated markedly with 50 μM indomethacine and this trend was continued through stimulation with 250 μM. (Bottom row) ARPE-19 cells were stimulated with indomethacine (250 μM) for the indicated time and subjected to the same analysis. Nrf2 in nuclear protein showed a time-dependent increase. On the other hand, HO-1 in cytosolic protein was showed maximal immunoreactivity at 12 h. (**b**; Top row) ARPE-19 cells were also stimulated with bromfenac for 3 h. Nrf2 was also upregulated in a dose-dependent manner. Increase of HO-1 in cytosolic protein was nearly the same as Nrf2 in nuclear protein. (Bottom row) Time-course expression of Nrf2 in nuclear protein and HO-1 in cytosolic protein with bromfenac (100 μM).

Figure 3c). Statistics were subjected to Mann–Whitney *U*-test with Bonferroni correction.

Reduction of Experimental CNV Size by Bromfenac in Rat Model

Our *in vitro* experiments showed that NSAIDs attenuated H_2O_2-induced RPE cell apoptosis. Next we examined the effects of bromfenac ophthalmic solution in a rat model of CNV. The size of CNV was measured with flat-mounted choroid stained with fluorescein dextran (Figure 4a). As shown in Figure 4b, CNV size was significantly smaller in bromfenac-treated eye ($32\,176 \pm 9165.1\ \mu m^2$) than in saline-treated rats ($48\,383 \pm 12\,733\ \mu m^2$; $P<0.001$, Mann–Whitney *U*-test).

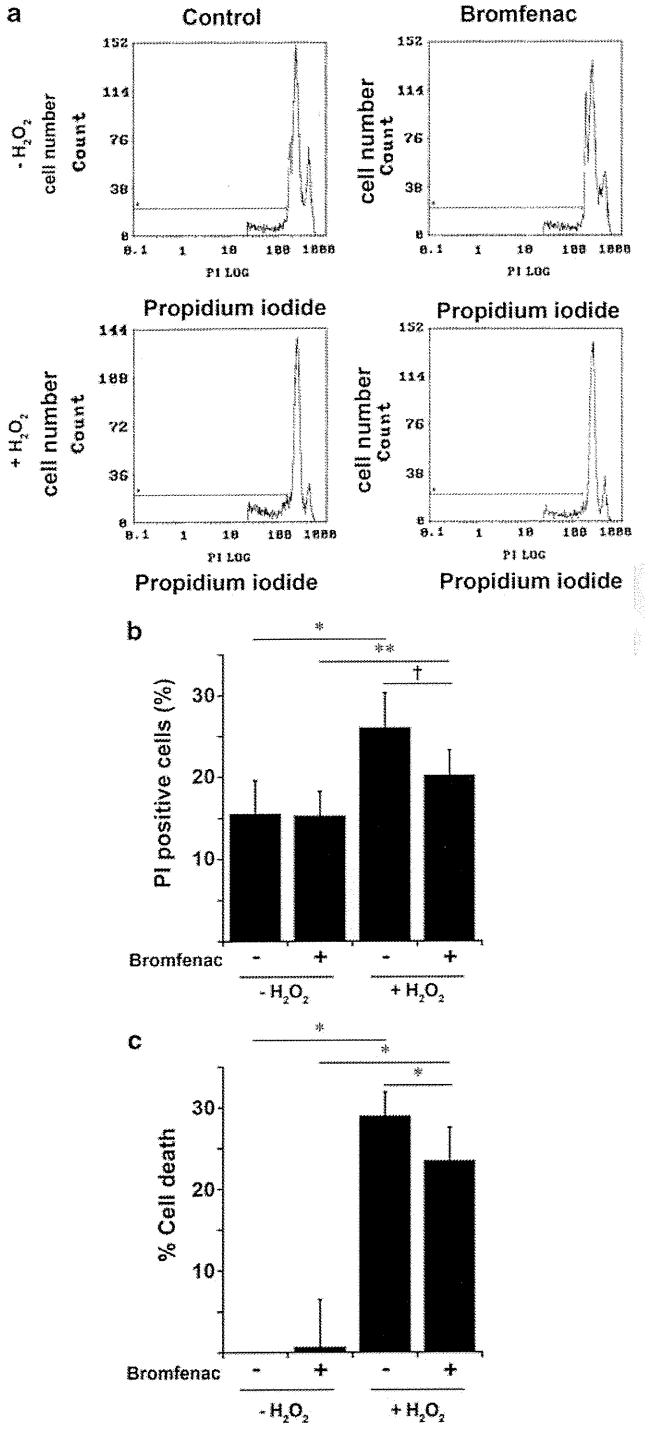

Bromfenac Upregulated Nrf2 and HO-1 in Experimental CNV

The size of experimental CNV was reduced by topical bromfenac. To examine the underlying mechanism, we evaluated expressions of Nrf2 and HO-1 in the CNV area. Our results *in vitro* showed Nrf2 was strongly stained in cell nucleus especially at and adjacent to the CNV area in rats that received bromfenac compared with the control rats. At the same time, expression of HO-1 was observed in cells at CNV lesions. Notably, HO-1 was also strongly found not only at the CNV area but also in the entire retina (Figure 5a and b). To identify the cell type to express HO-1 in bromfenac-treated eyes, the eyes were double stained using anti HO-1 antibody and antibodies specific to each cell type. Anti-RPE65 antibody for RPE cells, anti-GFAP antibody for glial cells, anti-ED1 antibody for macrophages, and anti-CD31 antibody for endothelial cells in the rat CNV model were treated with bromfenac. HO-1 were obviously co-stained with RPE65, GFAP, ED1 antibodies (arrows), implying that RPE cells, GFAP-positive cells (astrocytes or Müller cells), and ED1-positive macrophages were strongly correlated with HO-1 production. HO-1 was also upregulated around

Figure 3 Anti-apoptotic effect of bromfenac was analyzed by flow cytometry. (**a**) ARPE-19 cells were pretreated with bromfenac (left lane) or DMSO (right lane) as a control for 24 h. Then, the cells were stimulated with (bottom) or without (top) 1 mM H_2O_2 for 3 h. After stimulation, the cells were stained with PI, and the DNA content was determined with a FACS analyzer. (**b**) H_2O_2 increased cell apoptosis in both DMSO-treated and bromfenac-treated cells (*$P<0.001$ and **$P<0.005$, respectively). Apoptosis induced by oxidative stress was significantly less in bromfenac-treated cells compared with DMSO-treated control cells ($^{\dagger}P<0.01$). Treatment with bromfenac itself resulted in no significant difference in apoptosis ($P=0.86$). Each group included results of 10 independent examinations ($n=10$). Data were expressed as mean ± s.e.m. The corrected significant *P*-value (Mann–Whitney *U*-test) was defined as 0.0125 (0.05/4 comparisons) after Bonferroni correction. (**c**) Cytoprotective effect of bromfenac was analyzed using MTT assay. ARPE-19 cells were pretreated with bromfenac or DMSO as control for 24 h. Then cells were stimulated with or without 500 μM H_2O_2 for 15 min. After stimulation, cells were incubated with MTT (0.5 mg/ml) for 3 h, formazan product was solubilized by DMSO, dehydrogenase activity was expressed as absorbance and % cell death was determined compared with control. H_2O_2 increased cell death in both DMSO-treated and bromfenac-treated cells (*$P<0.001$). Cell death induced by oxidative stress was significantly less in bromfenac-treated cells compared with DMSO-treated control cells (*$P<0.001$). Treatment with bromfenac itself made no significant difference in cell viability ($P=0.519$). ($n=16$). Data were expressed as mean ± s.e.m. The corrected significant *P*-value (Mann–Whitney *U*-test) was defined as 0.0125 (0.05/4 comparisons) after Bonferroni correction.

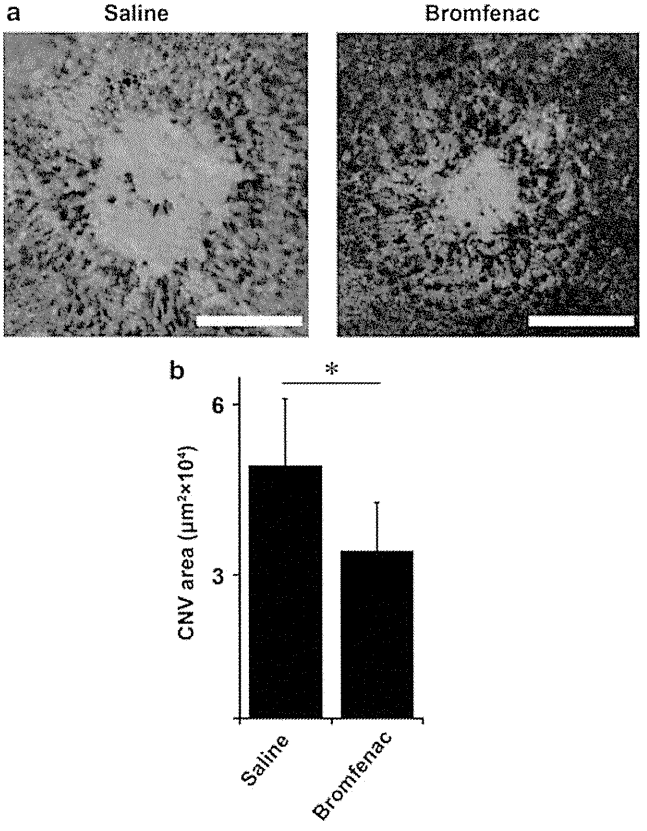

Figure 4 Size of CNV was examined after bromfenac treatment. (**a**) Representative CNV lesions of CNV flat mounts. Scale bars: 200 μm. (**b**) An analysis of the sizes of CNV lesions 8 days after PC. CNV size is smaller in bromfenac eye drop-treated rats $32\,176 \pm 9165.1\,\mu m^2$ than saline eye-drop treated rats $48\,383 \pm 12\,733\,\mu m^2$ (*$P<0.001$, Mann–Whitney *U*-test). $n=40$ (40 PC spots of 10 rats). Data were expressed as mean ± s.e.m.

CD31-positive blood vessels, but less co-staining was observed compared with RPE cells or GFAP-positive cells (arrowheads; Figure 5c).

We also examined the protein quantity of Nrf2 and HO-1 using homogenates of retina and choroid of rat CNV model. Western blot analysis showed no immunoreactivity to Nrf2. It is more than probable that the concentration of Nrf2 in the prepared nuclear extract was too low to be detected. Western blot analysis of cytosolic extracts showed that HO-1 was upregulated in the tissue of rat treated with bromfenac as observed in immunohistochemical analysis (Figure 6a). An analysis using densitometry of five independent western blot results confirmed upregulation of HO-1 in bromfenac-treated eyes and photocoagulated (PC) eyes (Figure 6b). Expressions of HO-1 in saline-treated eyes with no PC were defined as base line, and fold increases of HO-1 in other eyes were calculated. Topical bromfenac significantly upregulated HO-1 expression (1.85 ± 0.19-fold, $P<0.01$), and bromfenac-treated eyes with PC expressed more significant HO-1 expression (2.21 ± 0.36-fold, $P<0.01$) compared with saline-treated eyes. Although there was no statistical significance, PC itself slightly upregulated HO-1 expression by 1.21 ± 0.24-fold).

HO-1 Inhibitor Stannic Mesoporphyrin (SnMP) Reversed Inhibitory Effect of Bromfenac on CNV

Upregulation of HO-1 by NSAIDs was observed both in our *in vitro* and *in vivo* experiments. We examined whether the inhibition of HO-1 changed the size of experimental CNV. Topical bromfenac decreased the size of CNV compared with the control (bromfenac rat $28\,191 \pm 5466\,\mu m^2$ *vs* control rat $42\,405 \pm 9004\,\mu m^2$ control: $P<0.001$). This inhibitory effect was diminished by intraperitoneal injection of SnMP (iSnMP; bromfenac rat $28\,191 \pm 5466\,\mu m^2$ *vs* bromfenac + iSnMP rats $44\,677 \pm 7619\,\mu m^2$, $P<0.001$ or control rat $42\,405 \pm 9004\,\mu m^2$ *vs* bromfenac + iSnMP rats $44\,677 \pm 7619\,\mu m^2$, $P=0.923$). On the other hand, iSnMP itself did not have any significant effect on CNV size ($44\,057 \pm 14\,775\,\mu m^2$; Figure 7).

Inhibitory Effect of Bromfenac on Macrophage Infiltration Was Diminished by SnMP

The above experiments revealed that topical bromfenac reduced the size of the CNV, and iSnMP reversed this reduction (Figure 8). To identify the mechanisms underlying this phenomenon, we measured the number of macrophages infiltrating into the CNV area. As a result, in the group which received intraperitoneal PBS (iPBS), infiltration of macrophage was significantly decreased in bromfenac-treated eyes compared with saline-treated eyes (18.0 ± 6.04 cells/field bromfenac + iPBS rats *vs* 32.4 ± 6.07 cells/field saline + iPBS rats; $P<0.01$). iSnMP reversed this effect and significantly increased macrophage infiltration (18.0 ± 6.04 cells/field bromfenac + iPBS rats *vs* 37.4 ± 4.28 cells/field bromfenac + iSnMP rats; $P<0.01$). There was no significant change with macrophage infiltration in saline-treated rats (31.0 ± 4.24 cells/field saline + iSnMP rats *vs*, 37.4 ± 4.28 cells/field bromfenac + iSnMP rats; $P=0.074$).

Reduction of Intraocular VEGF by Bromfenac Was Diminished by SnMP

The amount of VEGF in ocular fluid obtained from the CNV model on day 8 was evaluated with ELISA. As a result, the amount of VEGF increased in CNV model in comparison with rat eyes without laser burn. VEGF level was significantly lower in bromfenac-treated rat than control CNV rats (1.09 ± 0.88 pg/mg protein bromfena + iPBS rats *vs* 3.08 ± 3.19 pg/mg protein saline + iPBS rats; $P<0.01$). Additional iSnMP increased intraocular VEGF level as high as that of control CNV rats (5.35 ± 4.23 pg/mg protein bromfenac + iSnMP rats *vs* 1.09 ± 0.88 pg/mg protein bromfenac + iPBS rats; $P<0.001$). No significant difference resulted from iSnMP itself (4.09 ± 3.87 pg/mg protein saline + iSnMP rats *vs* 3.08 ± 3.19 pg/mg protein saline + iPBS rats; $P=0.499$; Figure 9).

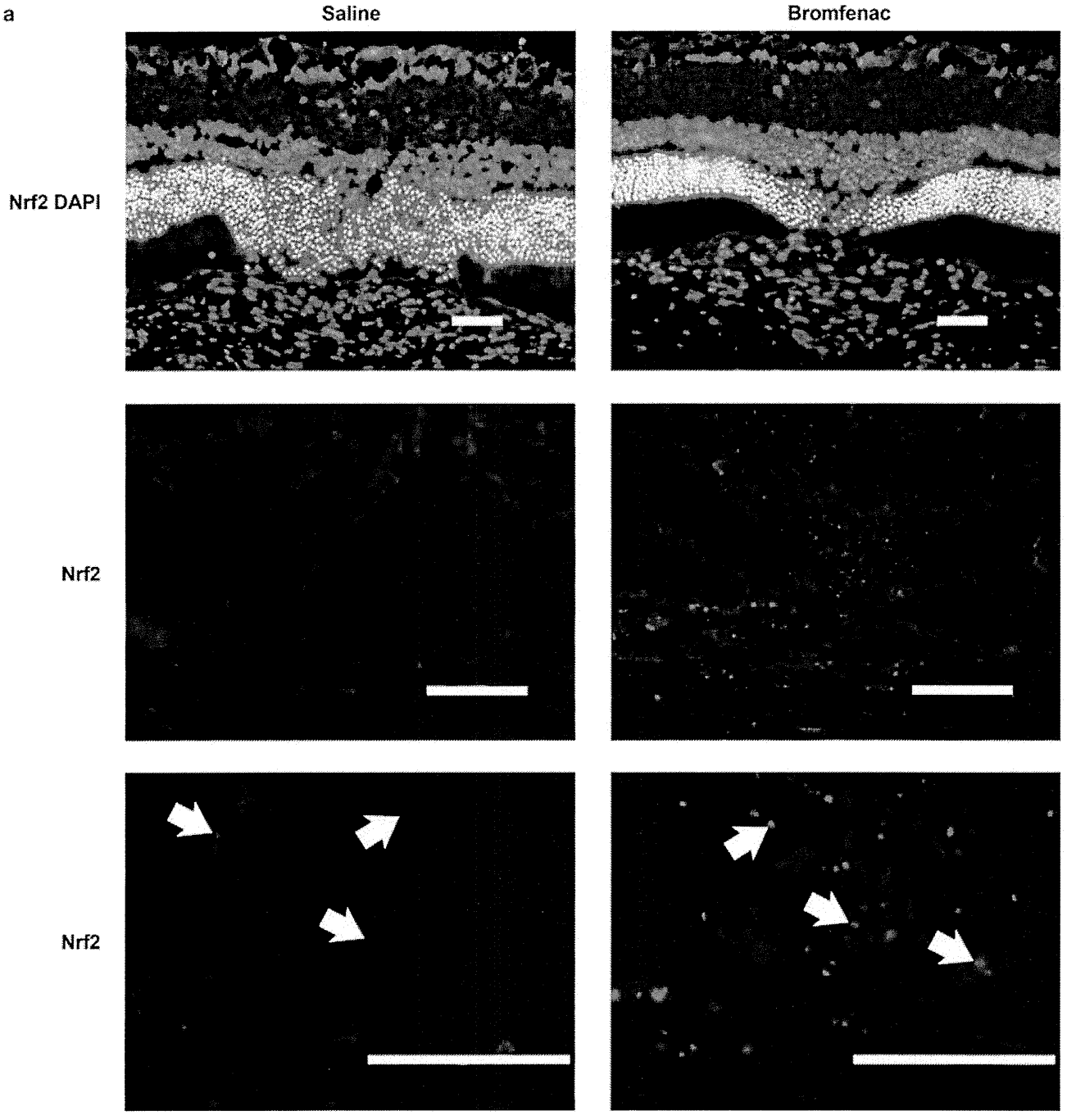

Figure 5 Immunohistochemical analysis was carried out for CNV lesions using Nrf2 or HO-1 protein. Immunofluorescent study was performed with anti-Nrf2 antibody (**a**) and anti-HO-1 antibody (**b**) in rat CNV model. Nuclei were counter-stained with 4′-6-diamidino-2-phenylindole (DAPI). (**a**) The results showed that expression of Nrf2 was upregulated and accumulated in cell nuclear especially at and near the CNV lesion (arrows). (**b**) Expression of HO-1 was also upregulated with bromfenac eye drop compared with saline-treated eye, especially at the photocoagulated CNV area and inner limited membrane (arrowheads). Scale bars: 100 μm. (**c**) Double staining for immunohistochemical analysis with anti-HO-1 antibody and cell-specific antibodies. Anti-RPE65 antibody for RPE cells, anti-GFAP antibody for glial cells, anti-ED1 antibody for macrophages, and anti-CD31 antibody for endothelial cells were in rat CNV model treated with bromfenac. HO-1 were obviously co-stained with RPE65, GFAP, ED1 antibodies (arrows), implying that RPE cells, GFAP-positive cells (astorcytes or Müller cells) and ED1-positive macrophages were strongly correlate with HO-1 production. HO-1 was also upregulated around CD31-positive blood vessels but less co-staining was observed compared with RPE cells or GFAP-positive cells (arrowheads). Nuclei were counter stained with DAPI. Scale bars: 100 μm.

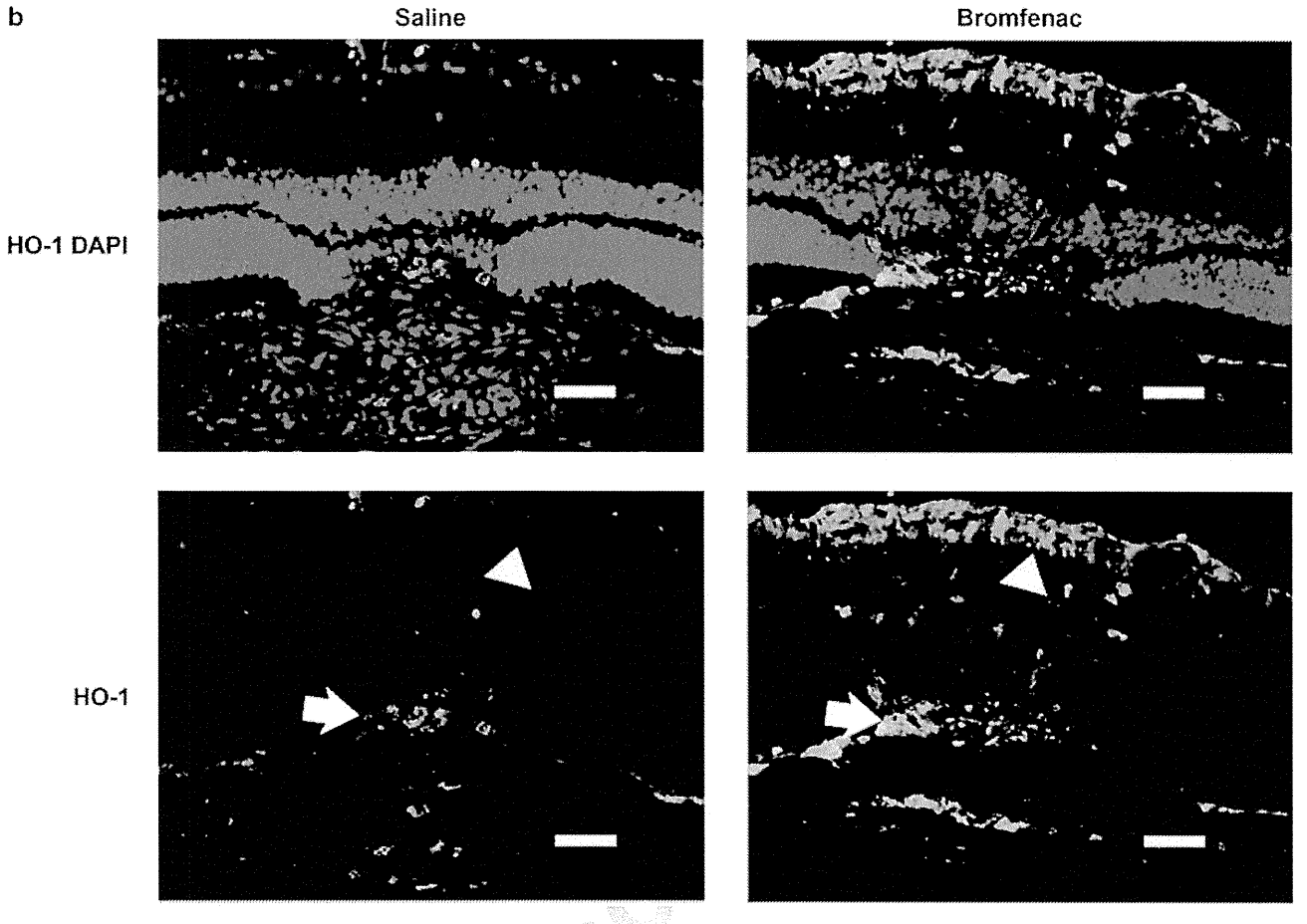

Figure 5 Continued.

DISCUSSION

Previously, we reported that intravitreous NSAIDs inhibited laser-induced CNV in sub-human primate; however, its mechanism was not well addressed.[11] Several recent reports showed possible mechanisms of the inhibitory effect of NSAIDs on CNV.[11–18] VEGF is one of the most potent molecules in angiogenesis. Takahashi *et al*[13] reported that nepafenac inhibited neovascularization in mice with CNV due to laser-induced rupture of Bruch's membrane and Kim *et al*[16] showed that ketrolac reduced the size of laser-induced CNV. Both suggested that the inhibitory effect of NSAIDs was due to downregulation of VEGF expression in the retina. Our previous study showed that blocking VEGF by gene transfer strongly inhibited CNV in this model.[31] Indeed, intraocular VEGF was significantly reduced in bromfenac-treated eyes in this study and thus inhibition of VEGF was also likely to have a crucial role in the inhibition of CNV formation found in this study.

There may be several explanations for the mechanism of this phenomenon. The first is the direct effect of NSAIDs on endothelial cells. It was reported that NSAIDs directly affect endothelial cells to down-regulate VEGF *in vitro*.[33,34] The targeted portions were supposed to be MAP kinase, ERK2 or the expression of VHL tumor suppressor protein, resulting in ubiquitination and degradation of HIF-1α.[33,34] Another report showed that NF-κB, which can also increase the expression of VEGF, and was inhibited by NSAIDs.[35] These direct mechanisms were probably at work in the present model, at least in part. The second is that the present phenomenon was caused by the inhibition of inflammation, which is an indirect effect. This explanation would be quite understandable because inflammatory cells are major sources of VEGF and depletion of macrophage strongly reduced the size of CNV, as demonstrated by ourselves and others.[36] NSAIDs were reported to reduce the prostaglandin, which is a known potent inducer of inflammation, in mouse retina.[14,16] Besides, NF-κB has a central role in the expression of various pro-inflammatory mediators and leukocyte infiltration.[37] So inflammation was inhibited by NSAIDs, consequently reducing the size of CNV. This is compatible with the present result that the number of macrophages infiltrating into the laser burned areas was significantly less in bromfenac-treated eyes than in PBS-treated controls.

In contrast, we shed light on another mechanism of NSAIDs in this study, ie, anti-stress protein in NSAIDs-mediated CNV suppression. Nrf2 is located at the cytosol binding to Keap1 under a stress-free condition; whereas after activation under the stressors, Nrf2 translocates to the

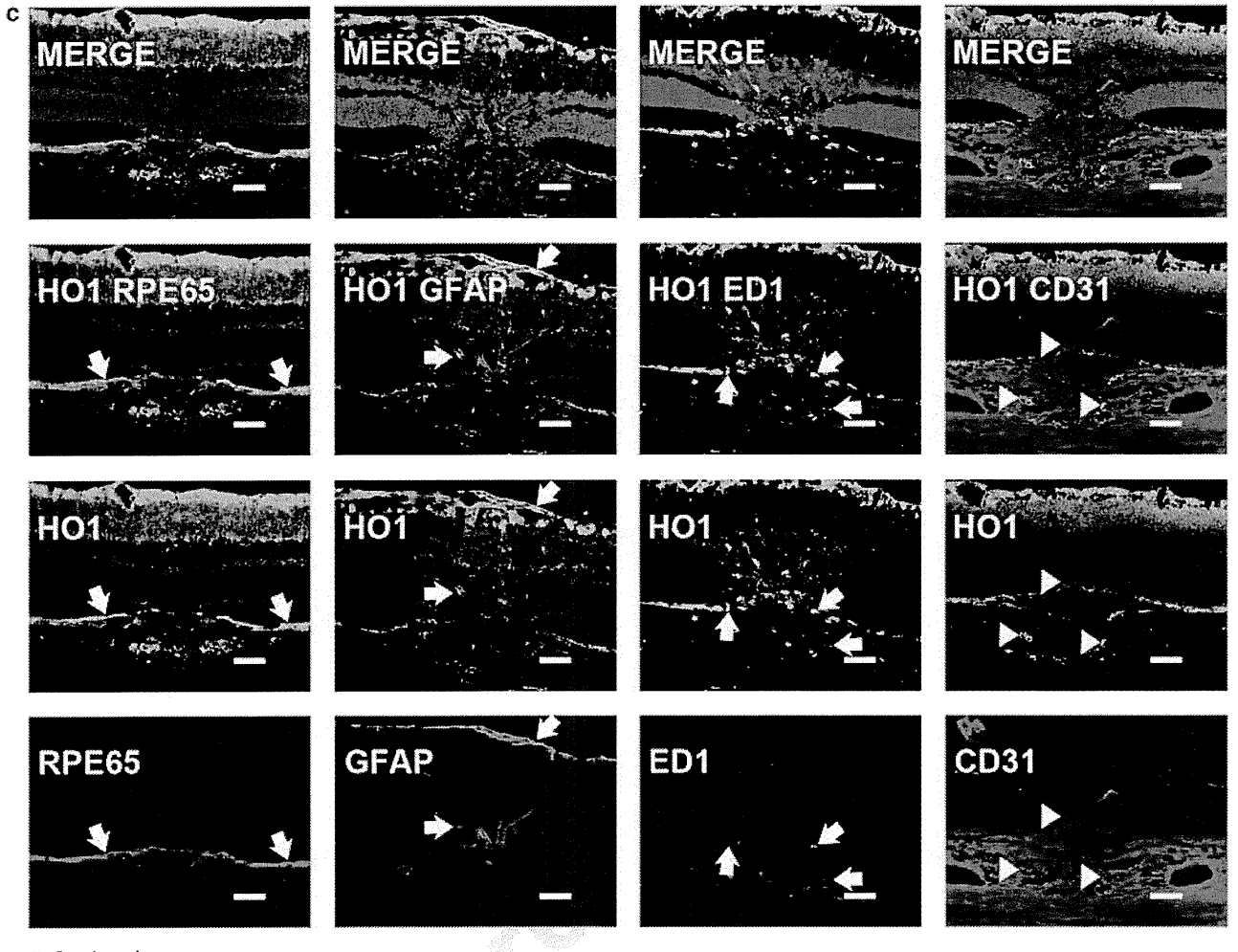

Figure 5 Continued.

nucleus, where it binds to the consensus *cis*-element (Maf-recognition element) to turn on the anti-oxidative stress mechanism, which can result in cell protection.[38,39] Because COX2 inhibits the activity of Nrf2, NSAIDs are supposed to activate the Nrf2/ARE pathways.[39,40] HO-1 is a phase II drug-detoxifying enzyme, such enzymes are regulated in a coordinated manner through a consensus *cis*-element and transcription factors, such as Nrf2. The present findings *in vitro* are consistent with this theory.

To our knowledge, this is the first report to show that NSAIDs induce HO-1 in the retina *in vivo* and *in vitro*. Interestingly, photocoagulation itself increased HO-1 expression in the retina, suggesting that HO-1 was induced by stress such as photocoagulation. However, HO-1 increased in bromfenac-treated eyes with no laser treatment and it was far more significant than in eyes with laser-burn alone. It is noteworthy that the inhibitory effect of bromfenac on CNV was diminished after the administration of SnMP. On the other hand, the size of CNV was not affected by saline eye drops after SnMP administration. These findings suggest that HO-1 does not necessarily have a pivotal role in CNV formation, but has a critical role in the inhibitory processes of bromfenac.

The role of HO-1 in angiogenesis is controversial.[41–43] It is suggested that during inflammation HO-1 has two different roles: first, an anti-inflammatory action inhibiting leukocyte infiltration; and second, promotion of VEGF-driven non-inflammatory angiogenesis, which facilitates tissue repair. In this study, bromfenac increased the expression of HO-1 associated with the inhibition of macrophage infiltration, whereas the inhibition of HO-1 by SnMP significantly augmented macrophage infiltration even in bromfenac-treated eyes. Thus, the increase of HO-1 expression by bromfenac was likely to lead to the inhibition of macrophage infiltration more than the promotion of VEGF-driven non-inflammatory angiogenesis in rat CNV model. Besides, our examination using intraocular fluids revealed that, bromfenac reduced the intraocular VEGF level (Figure 9). Consequently, CNV was inhibited.

Another important impact of HO-1 on retinal cells is its protective role, which was also observed as in the present *in vitro* study. In the *in vivo* study for example, curcumin